CHAPTER 4: Acclimation of maize source leaves to CO$_2$ enrichment at flowering

4.1   Abstract

As an extension of the study on maize acclimation to high CO2 initiated in Chapter 3, a further study was launched to identify additional morphological and photosynthetic changes, and, in particular, the effect of CO2 ennrichment on the maize transcriptome. To this end maize plants grown for 8 weeks under either air (350µl l^{-1} CO$_2$) or high CO$_2$ (700µl l^{-1} CO$_2$) were studied. Whole plant morphology was unaffected by high CO$_2$ under the growth conditions used in this part of the study in contrast to previous results. Photosynthesis was decreased on a surface area basis as a result of CO$_2$ enrichment but relatively few changes in transcripts involved in photosynthesis and related metabolism were observed. Transcriptome comparisons revealed over 3000 transcripts modified between leaf ranks 3 (old source leaves) and 12 (young source leaves) but only 142 and 90 transcripts respectively were modified as a result of high growth CO$_2$ availability. The high CO$_2$ leaf transcriptome displayed a decreased oxidative stress signature with effects on primary metabolism largely restricted to the youngest source leaves. Among the up-regulated transcripts two novel CO$_2$-modulated putative serine protease inhibitors (a serpin and a Bowman-Birk-type inhibitor) were identified, which were modulated by both sugars and pro-oxidants. High CO$_2$ decreased leaf protein carbonyls, which were most abundant in the young source leaves. The oldest source leaves were virtually free of protein carbonyls in air but were rich in hexoses. Growth with high CO$_2$ decreased protein carbonyl formation and eliminated development-dependent changes in the leaf hexose accumulation. It's concluded that the control of leaf hexose accumulation during leaf development is the most important factor modulating the two putative serpin and Bowman-Birk inhibitor transcripts in response to CO$_2$ enrichment *in planta*.

4.2   Introduction

The on-going substantial rise in atmospheric CO_2 levels presents multiple challenges for the sustainable management of agricultural ecosystems. While photosynthesis is considered to play a crucial role in ecosystem sustainability (Millennium Ecosystem Assessment, 2005) major uncertainties remain concerning high atmospheric CO_2-dependent effects on the relative competitiveness of plants using the C_3 and C_4 pathways of photosynthesis (Ward et al., 1999: Wand et al., 1999; Zhu et al., 1999). The CO_2-concentrating mechanism employed by C_4 plants diminishes CO_2-limitations at the active sites of RuBisCO, leading to suggest that C_4 plants will not respond positively to rising levels of atmospheric CO_2. However, the acclimation of photosynthesis involving down-regulation of RuBisCO and the Benson-Calvin cycle that has often been observed when C_3 species are grown with atmospheric CO_2 enrichment may be absent from C_4 plants, where these enzymes have already acclimated to functioning under high CO_2 conditions. Literature evidence suggests that different C_4 plants such as *Amaranthus retroflexus*, maize, *Sorghum bicolour,* and *Paspalum dilatatum* can benefit from increased atmospheric CO_2 availability, showing enhanced rates of photosynthesis (Maroco et al., 1999; Ziska and Bunce, 1999; Ward et al., 1999; Cousins et al., 2001) and carbon gain (Driscoll et al., 2006; Soares et al., 2008). However, the degree of the response of photosynthesis to CO_2 enrichment varies between species and conditions such that often little or no effect is observed (Sage, 1994; Ghannoum et al., 1997 and 2001; von Caemmerer et al., 2001, Wand et al., 2001; Leakey et al., 2006).

Atmospheric CO_2 availability exerts a strong influence on leaf structure and composition as well as stomatal density and patterning (Larkin et al., 1997; Croxdale, 1998; Taylor et al., 1994; Masle, 2000; Lake et al., 2001; 2002; Poorter and Navas, 2003; Martin and Glover, 2007). The stomatal index increased in response to CO_2 in maize (Chapter 2) and *P. dilatatum* (Soares et al., 2008), two monocotyledonous C_4 species, implying that fewer epidermal cells surround each stomatal aperture. The CO_2-signalling pathways that orchestrate these changes in leaf structure and composition responses remain poorly characterised (Gray et al., 2000; Ferris et al., 2002) but signals transported from mature to developing leaves are considered to be important regulators of such responses (Coupe et al., 2006; Miyazawa et al., 2006).

While the regulation of photosynthesis and related gene expression has been extensively characterized with respect to CO_2 availability in dicotyledonous C_3 leaves, little information is available on the effects of CO_2 enrichment in C_4 plants. The focus of this research has therefore been to elucidate how metabolism and gene expression in the different leaf ranks of maize at anthesis, a point where all the leaves are source leaves, respond to growth with CO_2 enrichment. Maize leaves are monocotyledonous species and employ the NADP-malic enzyme (ME) decarboxylation pathway of C_4 photosynthesis. In the present study, a classic whole plant physiology approach has been combined with molecular genetic techniques to resolve the genetic basis for the responses of maize to the rise in atmospheric CO_2, which could be almost double the 2006 figure of $381 \mu l \ l^{-1}$ in 2050. Any estimation of the role of C_4 photosynthesis in sustaining both cultivated and natural ecosystems (Millennium Ecosystem Assessment, 2005), necessitates an improved understanding of how leaf metabolism and gene expression are controlled in C_4 plants, particularly at flowering, a stage which is very sensitive to water deprivation and other environmental stresses.

Since very little information is available in the literature on the components that regulate leaf protein turnover in response to CO_2 enrichment, the effect of development and CO_2 enrichment on maize plants was investigated, focusing on the leaf transcriptome and leaf metabolism. A further aspect of this study was to investigate if CO_2 enrichment also affects the function of proteases and their inhibitors in maize plants. In order to characterize the metabolic components that are important in the regulation of leaf proteases and protease inhibitors, the respective roles of carbohydrate status and cellular oxidation state in the regulation of gene expression and protein turnover with respect to growth CO_2 level were investigated.

4.3 Materials and Methods

All methods were performed by A. Prins, unless otherwise indicated.

4.3.1 Plant material and growth conditions

Zea mays L. hybrid H99 plants were grown for eight weeks in compost (Driscoll et al., 2006) in duplicate controlled environment rooms (Sanyo 970, SANYO, Osaka) where the atmospheric CO_2 was maintained at either $350 \mu l \ l^{-1}$ or at $700 \mu l \ l^{-1}$. The plants were

exposed to 16h photoperiod (700μmol m^{-2} s^{-1}) and the temperature was maintained at 25ºC (day) and 19ºC (night) with 80% relative humidity. The CO_2 was supplied from a bulk container, transmitted via a Vaisala GMT220 CO_2 transmitter (VAISALA OYJ, Helsinki, Finland), and maintained by a Eurotherm 2704 controller (EUROTHERM LTD., Worthing, U.K.) that kept CO_2 levels at 350 ± 20μl l^{-1} or 700 ± 20μl l^{-1}. All plants were watered everyday throughout development in order to avoid a water stress, especially in plants grown at 700μl l^{-1}.

4.3.2   Growth analysis

The following measurements were performed at the 12-13 leaf stage (8 weeks) from plants grown either in air or at high CO_2 (Fig. 4.1). In all experiments leaf phylogeny was classified from the base to the top of the stem, leaf one being at the bottom and leaf twelve at the top. Measurements were performed sequentially as follows:
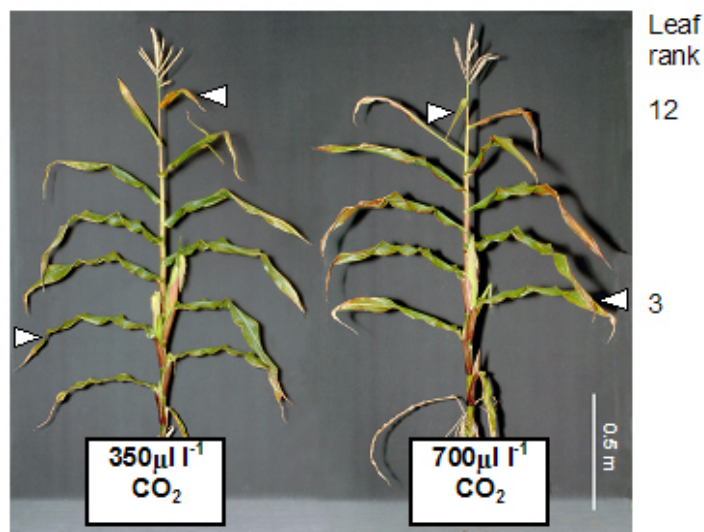

Figure 4.1 A comparison for the air (350μl l^{-1}) and high CO_2 (700μl l^{-1}) maize phenotypes at 8 weeks. The leaf ranks sampled for microarray analysis are indicated by arrows.

i) Leaf weight and area

The fresh weight and area of each leaf was measured following excision. Total leaf fresh weights were determined on a standard laboratory balance. Leaf area was measured using a ΔT area meter (Delta-T Devices LTD, England) according to instructions of the manufacturer.

ii) Tissue water content

Tissue water contents were determined from the relative fresh weight and dry weights of $8cm^2$ leaf disks. Discs were harvested from the centre of every second leaf, midway between leaf tip and base. Fresh weights were determined as above. The discs were then placed in an oven at 60°C for 3 days, after which time the discs were weighed again. Tissue water content was calculated according to the equation: tissue water content (TWC) = (fresh weight – dry weight) / dry weight.

4.3.3   Leaf tissue anthocyanin pheophytin, and chlorophyll contents

Anthocyanin was measured in maize samples according to Sims and Gamon (2002). Whole leaves from three biological replicates were pooled and ground until homogeneity with a pestle in a mortar, under liquid nitrogen, after which samples were stored in 50ml Falcon tubes at –80°C. Samples representing each leaf on the stem of maize plants grown either at $350\mu l\ l^{-1}$ or $700\mu l\ l^{-1}$ CO_2 were analysed. Aliquots of the pooled, homogenised leaf material (approximately 100mg) was crushed with liquid nitrogen in extraction solution (1ml; methanol/HCl/water [90:1:1, vol:vol:vol]) and ground until homogenised. Mortars were rinsed with an additional 1ml extraction solution which was added to the same tube, to ensure complete recovery of tissue. Due to the interference of pheophytin, which has an overlapping tail that absorbs light at A_{529}, an adjusted absorbance was calculated to obtain a corrected value from which anthocyanin content was calculated. Corrected absorbance was calculated using the following equation: corrected anthocyanin absorbance = A_{529} – (0.288 A_{650}). The corrected anthocyanin absorbance was used to calculate total anthocyanin content using a molar absorbance coefficient for anthocyanin at 529nm of 30,000 $M^{-1}\ cm^{-1}$ and using the Beer-Lambert equation: A = ε.C.L, where A – absorbance, ε - molar absorbance coefficient ($M^{-1}\ cm^{-1}$), C – concentration (M), and L – path length (cm). Anthocyanin content was expressed as nmol anthocyanin mg^{-1} pheophytin.

In acidified solutions used for measuring anthocyanin content the chlorophyll degradation product pheophytin was measured according to Vernon (1960). Absorbance of extracts prepared as described above was measured in a spectrophotometer at wavelengths of 655nm and 666nm. Pheophytin content of these solutions was calculated using the equation: pheophytin (mg l^{-1}) = 26.03 x A_{655} + 6.75 x A_{666}. Absorbance measurements for

pheophytin were taken in the same solutions in which anthocyanin content was determined, where pigments were extracted in a solution consisting of methanol/HCl/water (90:1:1, vol:vol:vol), and also after re-extraction of pelleted plant material collected after measurement of anthocyanin. For re-extraction, pelleted plant material was resuspended in 80% acetone and incubated overnight at -20°C in the dark. The values obtained in both solutions at 655nm and 666nm were added before calculating the final amount of pheophytin in the extract.

4.3.4 Quantification of leaf sucrose, hexose and starch

Quantification of leaf sucrose, hexose, and starch was performed by J. Muchwezi (University of Pretoria). Whole leaves were harvested and immediately frozen in liquid nitrogen in the growth cabinets. Hexose content was measured in frozen, crushed tissue pooled from three biological replicates, representing each leaf of the plant profile, according to Jones et al. (1977). Starch was extracted and assayed in the same samples according to the method of Paul and Stitt (1993). Sugar and starch content was expressed per µg chlorophyll.

4.3.5 Protein carbonylation

Protein carbonylation was determined by J. Muchwezi (University of Pretoria). Whole leaves were harvested and immediately frozen in liquid nitrogen in the growth cabinets. The composition and extent of protein carbonyl group formation was measured using the OxyBlot™ Oxidized Protein Detection Kit (Chemicon International, UK). Oxidative modification of proteins introduces carbonyl groups into the side chains of these proteins. Carbonyl groups can be derivatised with 2,4-dinitrophenylhydrazine (DNPH) and then detected by antibodies specific to the attached DNP moiety of the proteins. In brief, protein extracts (15-20µg) were first denatured by the addition of 6% SDS (v/v; total volume of 10µl) and then incubated in an equal volume of 1xDNPH for 15min at room temperature. Samples were neutralised by the addition of 7.5µl neturalisation buffer before being separated by SDS-PAGE. Proteins separated on the PA gel were transferred to a nitrocellulose membrane which was then incubated for 1h in blocking/dilution buffer. The membrane was then incubated for 1h in primary antibody diluted in blocking/dilution buffer to a concentration of 1:150. After washing the membrane three times in 1x phosphate buffered saline (PBS) it was incubated for 1h in secondary antibody diluted in

blocking/dilution buffer to a concentration of 1:300. The membrane was again washed three times with 1xPBS before being treated with chemiluminescent reagents and exposing the resultant membranes to X-ray film.

4.3.6 RNA extraction, purification, and analysis

Total RNA was extracted using Trizol reagent (Invitrogen, UK). This is a mono-phasic solution of phenol and guanidine isothiocyanate which protects RNA from degradation by inhibiting RNAse activity while disrupting cells and dissolving cell components. All solutions used throughout the procedure were treated with 1mM diethyl pyrocarbonate (DEPC) and autoclaved for 20min to remove RNase activity. In general, 300mg leaf tissue was ground to a fine powder in a mortar with pestle, in the presence of liquid nitrogen and then further homogenized with 3mL Trizol reagent. The sample was ground continuously until it had completely thawed. After 5min at room temperature the sample was centrifuged at 12000xg for 15min. The supernatant was extracted twice in chloroform (first in 0.2 volumes chloroform and then in an equal volume chloroform) by vortexing for 15 seconds after addition of chloroform, leaving samples at room temperature for 5min and then centrifuging at 8000xg for 10min. Addition of chloroform followed by centrifugation separates the solution into an aqueous phase and an organic phase. RNA is present exclusively in the aqueous phase. After transfer of the aqueous phase, the RNA was precipitated by the addition of 0.5 volumes isopropyl alcohol and incubation at room temperature for 30min. Precipitated RNA was sedimented by centrifuging at 12000xg for 10min and then washed in absolute ethanol (75%). The supernatant was discarded and the RNA pellet evaporated to dryness in a dessicator before re-suspension in DEPC treated water (100μl).

RNA concentration and purity was quantified by applying 2μl of dissolved RNA to the column of a NanoDrop ND-1000 spectrophotometer (NanoDrop Technologies, UK) and measuring the absorbance at 230nm, 260nm, and 280nm. An A_{260}/A_{280} ratio of ~2.0 and A_{260}/A_{230} ratio of 1.8-2.2 indicates RNA mostly free from contaminating substances. A ratio that is appreciably lower indicates the presence of proteins, phenol, or other contaminants in the former and co-purified contaminants in the latter. After spectrophotometric analysis, 40 - 100μg RNA from each sample was purified with RNeasy Mini Spin Columns (Qiagen) according to the manufacturers' instructions. After

purification, concentration and purity was again determined on the Nanodrop spectrophotometer. Quality of RNA samples was also determined by electrophoresis on agarose gels and staining with ethidium bromide, which allows the visualisation of the 18S and 28S ribosomal RNA (rRNA) subunits. A theoretical ratio of 1.7-2.0 between 28S and 18S indicates intact RNA, however, this ratio is difficult to attain in standard RNA isolation procedures. For electrophoresis, RNA samples (2μg) were heated to 65°C for 5min in a loading buffer containing 50% (v/v) glycerol, 1xTAE buffer, 1% (w/v) bromophenol blue and 60% (v/v) formamide before being cooled and then separated on a 1.5% non-denaturing agarose gel according to the method of Sambrook et al. (1986). Formamide is a denaturing agent that stabilizes RNA and ensures RNA molecules migrate according to size even in non-denaturing electophoresis. Agarose gels were run at 180V and 100mA to separate the RNA. RNA was visualised by including the fluorescent, intercalating agent, ethidium bromide in the gel and illuminating the gel with UV light after electrophoresis.

For the microarray study, leaf 12 (young leaf) and leaf 3 (old leaf) of 8 week-old maize plants grown at 350μl l^{-1} or 700μl l^{-1} CO_2 were used. Eight plants from each treatment were sampled, with equal amounts of RNA from 2-3 plants being pooled to obtain 3 replicate samples. For qPCR, RNA was extracted from pooled samples (n=3) of plants grown in either air or with CO_2 enrichment, representing each leaf on the stem (Fig. 4.2 A). For the feeding study, total RNA was extracted from 400mg of frozen tissue (Fig. 4.2 B).
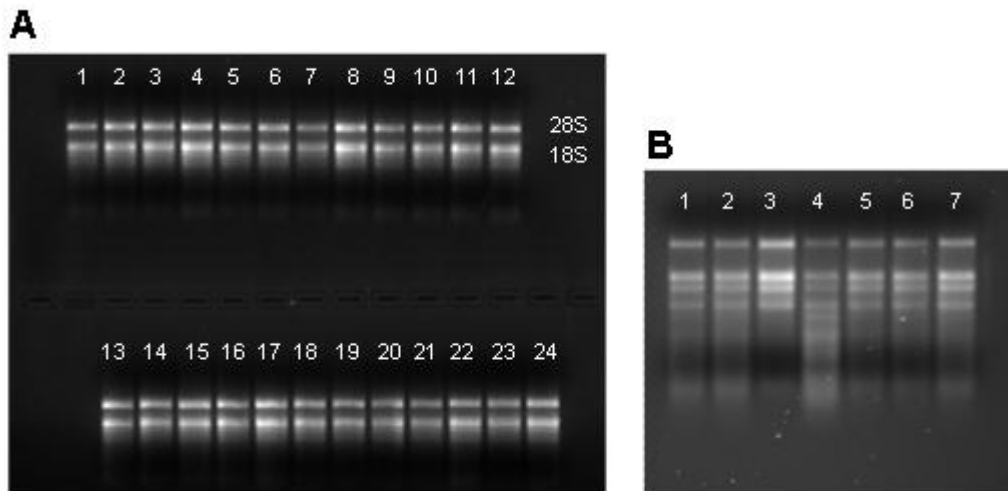
Figure 4.2 Electrophoresis of total RNA (2µg) on a 1.5% non-denaturing agarose gel visualized under UV after staining with ethidium bromide. RNA extracted from leaf 1 to leaf 12 for qPCR (A) of plants grown at 350µl l^{-1} CO_2 (1-12) or 700µl l^{-1} CO_2 (13-24), and RNA extracted from leaves after 16h of feeding (B) with 1) 10mM Hepes (pH7), 2) 1mM methyl viologen, 3) 20mM H_2O_2, 4) 20mM DTT, 5) 50mM glucose, 6) 50mM fructose, and 7) 50mM sucrose as detailed in section 4.6.

4.3.7 Micorarray hybridization

Three replicate samples of purified RNA from 8 biological replicates (2-3 biological replicates being pooled into a single sample) were used for microarray analysis. RNA was extracted from young (leaf 12 of 13) or old leaves (leaf 3 of 13) of maize plants grown either in air or with CO_2 enrichment, and sent to ArosAB, Denmark for microarray analysis. There, samples were converted to cDNA with Superscript (Invitrogen) and used to synthesise biotin-labelled cRNA (BioArray High Yield RNA Transcript Labeling Kit, Enzo). Labelled cRNA was fragmented before being hybridised to microarray chips (Affymetrix). This was done in triplicate for each sample. Each array was washed and scanned in a GeneChip Scanner 3000 (Affymetrix). The Affymetrix maize microarray chip provides comprehensive coverage of over 100 cultivars present in NCBI's UniGene data set with sequence information being selected from NCBI's GenBank [©] (up to September 29, 2004) and *Zea mays* UniGene Build 42 (July 23, 2004) databases. The array includes 17 555 probe sets for approximately 14 850 *Zea mays* transcripts which in turn represent 13 339 genes (12 113 of which are presented in distinct UniGene clusters).

4.3.8 Microarray analysis

Raw intensity values from the scanned array were analysed by P. Verrier (Rothamsted Research, UK) using the Robust Multichip Average method (RMA) (Bolstad et al., 2003)

as implemented in RMAExpress (http://rmaexpress.bmbolstad.com/). Normalised intensity values expressed as $\log_2$ values were compared as ratios, where a ratio of ±0.5 was selected as significant for further study. The putative identity of unknown or uncharacterised differentially expressed transcripts was determined by A. Prins. Putative transcript identity was determined from annotation available for probes at the NetAffx website (https://www.affymetrix.com/analysis/netaffx/index.affx),according to the Unigene cluster they fall into (http://www.ncbi.nlm.nih.gov/UniGene; Pontius et al., 2003), or by translated homology search. Homology search was done by translating the differentially expressed transcript sequence into amino acids (in all possible reading frames) and comparing it to known protein sequences (tblastx) on the NCBI protein refseq database (as on 17 March 2006) and the trembl (EBI) data set (as on 16 May 2006) with a criteria of minimum homology of 50% and e value of ≤-7 for significance.

4.3.9 Modulation of tissue sugars and redox state by exogenous supply of sugars and pro-oxidants

Leaf 3 (n=10) was removed from 3 week-old maize plants (seventh leaf emergent), cut into ~$1cm^2$ pieces under 10mM Hepes, pH7 and mixed well. Thirty of these pieces were placed into separate feeding solutions consisting of 50mM fructose, 50mM glucose, 50mM sucrose, 20mM DTT, 20mM H_2O_2, or 1mM methyl viologen in 10mM Hepes buffer, pH 7, and left for 16h in the dark. Feeding solutions were then drained, leaf pieces briefly dried by touching to paper towel, and RNA extracted (Fig. 4.2) for qPCR to quantify relative expression of selected transcripts. Controls consisted of leaf pieces incubated in 10mM Hepes buffer, pH 7 without addition of an extra solute.

4.3.10 Quantitative realtime PCR (qPCR) analysis
i) Selection of sequences for analysis and primer design
Transcripts were selected for further analysis by qPCR based on microarray results that revealed an effect of CO_2 enrichment or developmental stage on them (Table 4.1). Two transcripts specifically modified by CO_2 (Zm.3332.1.A1_at and Zm.4270.2.A1_a_at) and 5 transcripts specifically modified by developmental stage (Zm.13430.1.S1_at; Zm.231.1.S1_at; Zm.3478.1.S1_a_at; Zm.6977.1.S1_at; Zm.26.1.A1_at) were analysed. Quantitative PCR was done, firstly, in each leaf of the maize plant profile and, secondly, after feeding leaves as detailed in section 4.3.9. Primers targeting a 50-53bp region on

Table 4.2. Expression values of endogenous controls based on microarray results. Probe sets with a raw expression intensity of >10 000 ($\log_2$ value = 13.288) were selected as endogenous controls.

Probe set and gene identity	$\log_2$ raw expression values				Forward primer	Reverse primer
	Old-Air	Young-Air	Old-CO_2	Young-CO_2		
Zm.12132.3.S1_a_at Ubiquitin	14.070	14.013	14.074	14.025	GTGCCTGCGTCGTC TGG	AACAGCAGATACT TTGACAACCTCC
Zm.719.1.A1_at Thioredoxin M	13.306	13.329	13.328	13.305	CATGCATCGACGAC TAAACACA	TGATCATATCCCGT ATGCAAAGG
AFFX-Zm_Cyph_3_at Cyclophilin	13.786	13.812	13.795	13.775	TCCGTTCCTTTGGA TCTGAATAA	AACTAAGACCACC ACTCAGATCACC

ii) Sequence amplification

Purified total RNA was extracted from samples pooled from three biological replicates for qPCR on the plant profile, and from 400mg frozen leaf tissue obtained from ten biological replicates for the feeding study using Trizol reagent (Invitrogen) as detailed in section 2.5.1. The purified RNA (2μg) was treated with DNAse I (2U; amplification grade) (Invitrogen) according to the instructions provided by the supplier, for removal of any remaining genomic DNA. DNAse I was inactivated by incubation at 65ºC for 10min, after which first strand cDNA was prepared in the same tube using SuperScript II (Invitrogen) according to instructions provided by the supplier. Oligo dT_{12-18} primers (1μg), dNTP mix (12.5nmol each of dATP, dGTP, dCTP, and dTTP), first strand buffer (1x, as supplied by manufacturer), and 11.4mM DTT were added to DNAse treated RNA and incubated at room temperature for 2min before adding 200U SuperScript II and incubating the reaction at 42°C for 90min. Samples were stored at –20°C. Oligo dT primers amplify mRNA molecules by binding to 3' poly-A tails.

Primer stock solutions (100μM) for individual primers were first prepared, after which stock solutions containing both forward (5μM) and reverse (5μM) primers were prepared in autoclaved distilled H_2O, for use in amplification reactions. First-strand RNA template was diluted 2-fold and stored in aliquots. Quantitative PCR was done at least in triplicate on this template using the Applied Biosystems 7500 Real Time PCR System and SYBR green as intercalating dye. The SYBR® Green JumpStart™ Taq ReadyMix™ for Quantitative PCR (Sigma, UK) was used for amplification. The ReadyMix solution contains 20mM Tris-HCl, pH8.3, 100mM KCl, 7mM MgCl2, 0.4mM each dNTP (dATP,

dCTP, dGTP, TTP), stabilizers, 0.05unit/ml Taq DNA Polymerase, JumpStart Taq antibody, and SYBR Green I. SYBR Green is a fluorescent DNA binding dye with excitation and emission maxima of 494nm and 521nm respectively. It binds all double-stranded DNA causing an increase in fluorescence throughout cycling as DNA is amplified. An Internal Reference Dye (Sigma) that is similar to 6-Carboxy-X-rhodamine (ROX) was included as internal reference dye. Each amplification reaction consisted of 50% (v/v) SYBR Green JumpStart Taq ReadyMix, 1% (v/v) Internal Reference Dye, 200nM each forward and reverse primers and 4μl template in a total volume of 25μl. A mastermix containing all ingredients except template was prepared and aliquoted into the wells of a 96-well PCR plate, after which template was added to each well. Negative controls consisted of reaction solution not containing template.

In order to determine the concentration of template RNA to use in amplification reactions, as well as to monitor the efficiency of the amplification reaction with the different primer pairs, optimisation was performed on template as prepared after first strand amplification in a dilution series consisting of 1x, 0.1x, 0.01x and 0.001x solutions of template. It was decided that template diluted 10x would be used for all amplification reactions and final calculations (Fig. 2.6). All amplifications were done at least in triplicate, including a water control reaction for each primer set.

The following thermal cycler profile was used:

Stage	Repetitions	Temperature	Time
1	1	50°C	02:00
2	1	95°C	10:00
3	40	95°C	00:15
		60°C	01:00

iii) Amplicon abundance analysis

Relative quantitative analysis of transcripts was performed with the Applied Biosystems Detection Software (SDS) v1.2.1 (Fig. 4.3 and 4.4). For analysis, a baseline was firstly selected to exclude the initial cycles of amplification in which little change in fluorescence can be detected (Fig. 4.3). Secondly, a threshold level in the detected increase of fluorescence was selected above the baseline and within the exponential growth region of the amplification curve. The point at which the threshold level intersects the amplification

plot defines the threshold cycle (Ct). The Ct is the key value in qPCR analysis and is defined as the fractional cycle number at which the fluorescence detected by the system passes the threshold level as determined by the user. This value is used to calculate relative abundance of transcripts.
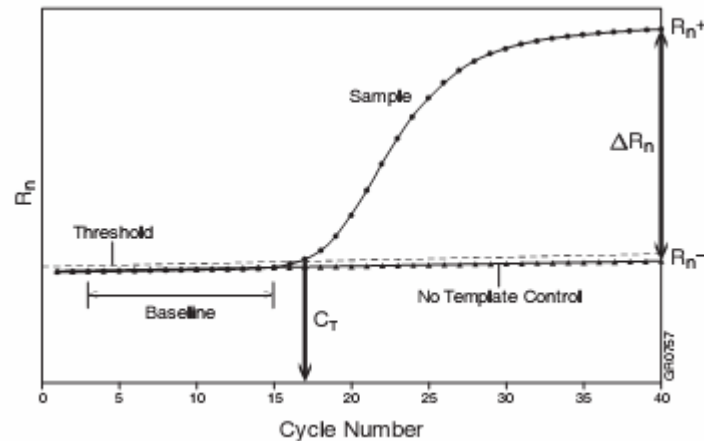

Figure 4.3 A representative amplification plot illustrating important parameters measured during qPCR (ABI7500 user manual).
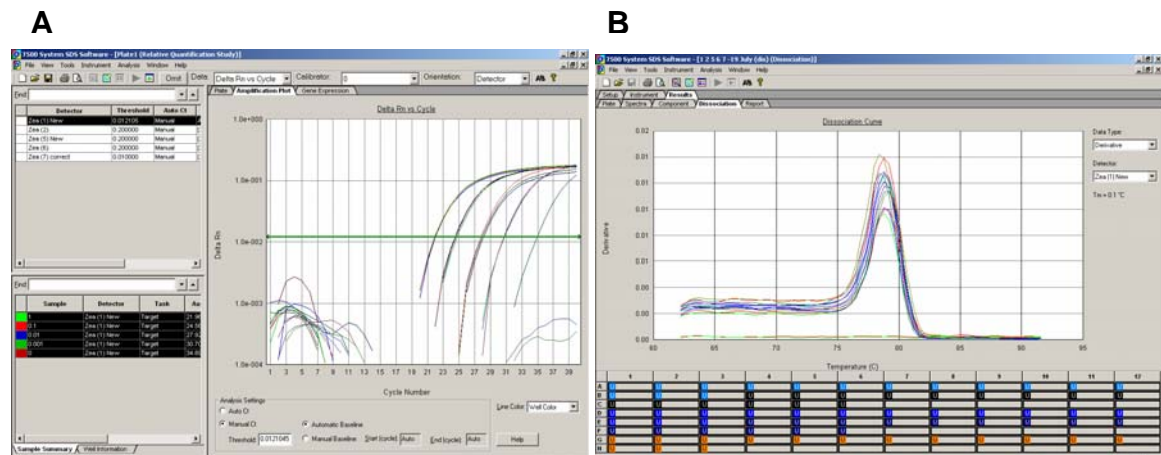

Figure 4.4 Example of amplification plot of a dilution series (A) showing change in fluorescence vs cycle number for template at 1x, 0.1x, 0.01x, and 0.001x concentration (represented from left to right on plot), and dissociation curve (B) of this reaction showing a single amplification product in a reaction where a putative serine protease inhibitor sequence was amplified.

Specificity of amplicons was confirmed by melting curve analysis (Fig. 4.4 B), where a single peak indicated a single amplification product, but multiple peaks indicated non-specific binding or contamination of reaction solution. Efficiency of individual amplification reactions was determined by first calculating the slope generated when graphing the Ct value of individual amplification reactions against a concentration series

of the template (expressed as a logarithm), and then using the equation Efficiency (E) = 10 $^{(-1/slope)}$. An efficiency of ≥ 2 represents acceptable amplification of template (Fig. 4.5) since it indiactes that each template strand produces two product strands during each amplification cycle.
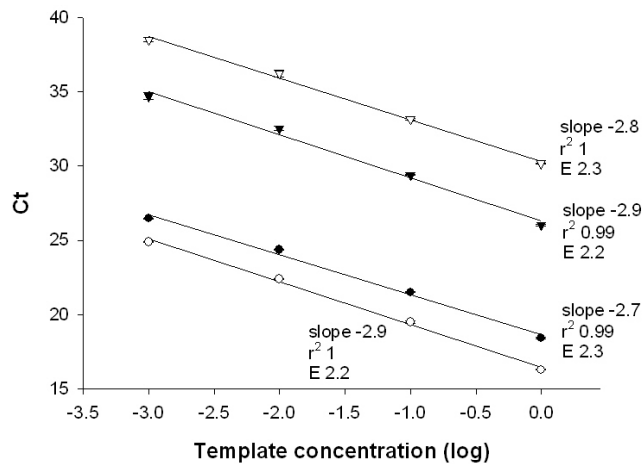

Figure 4.5 Example of amplification efficiencies obtained with primers designed to amplify invertase (open triangle), cell wall invertase (closed triangle), ubiquitin (closed circle), and thioredoxin (open circle) amplicons, showing the slope, r^2 value of regression line, and efficiency (E) calculated for each.

Relative abundance of qPCR amplicons were confirmed by comparison to the abundance of at least two endogenous controls. During qPCR analysis of transcript abundance in the maize leaf profile, leaf 1 (lowest on the stem) from air-grown plants was chosen as calibrator, and assigned a relative quantity (RQ) value of 1. The abundance of transcripts in other leaves was compared relative to this value. If a specific transcript was more abundant in a leaf relative to the abundance of that transcript in leaf 1, the RQ would be represented with a calculated value higher than 1. If a specific transcript was less abundant in a leaf relative to the abundance of that transcrtip in leaf 1, the RQ would be represented with a calculated value lower than 1. During analysis of transcript abundance after feeding of maize leaf pieces, leaf pieces fed only on 10mM Hepes, pH7 (with no added solute) was employed as calibrator, and assigned a RQ of 1.

4.3.11   Isolation and analysis of gene sequences of two novel protease inhibitors
i) Isolation of full-length protease inhibitor sequences
G. Beyene (University of Pretoria) performed determination of full-length gene sequences of two transcripts affected by CO_2 enrichment. Total RNA was extracted from leaf 3

pooled from seedlings (n=6) at five-leaf stage using the TriPure total RNA isolation kit according to the manufacturer's recommendation (Roche, Germany) and contaminant genomic DNA was digested by RNase-free DNase. Two μg of total RNA was reverse transcribed using superscript III™ Reverse Transcriptase (RT) (Invitrogen, USA) according to the manufactuer's instruction and used as a template in PCR reaction. Full-length cDNA clones for *Zea mays* putative serine-type endopeptidase inhibitor and putative Bowman-Birk-type serine protease inhibitor (accession numbers EF406275 and EF406276 respectively) were obtained by performing 5' and 3' rapid amplification of cDNA ends (RACE) using the GeneRacer™ kit according to the manufacturer's instruction (Invitrogen, USA) along with gene-specific primers. Gene-specific primers forward 5'-tactcagctcaaggttgaaggcatgg–3' and reverse 5'-cgaatcacgcacactttggttcagag-3' were used for isolation of a full-length serine-type endopeptidase inhibitor and primers forward 5'-cctcagctgatactcgtcggcact-3' and reverse 5'-gaacgtcgtcacagcggtaggtga-3' were used for isolation of a full-length Bowman-Birk-type serine protease inhibitor. The 5' RACE, 5' nested, 3' RACE and 3' nested primers were provided with the GeneRacer™ kit (Invitrogen, USA) that were used together with the gene specific primers. All amplified PCR products were T/A cloned into PCR4-TOPO (which was also provided with GeneRacer Kit) and sequenced in both direction using M13 forward and reverse primers.

Sequencing of the inserts were performed by using the BigDye® Terminator Cycle Sequencing FS Ready Reaction Kit, v 3.1 on ABI PRISM® 3100 automatic DNA-Sequencer (Applied Biosystems, USA). The BLASTn and BLASTp programs (Altschul et al., 1997) were used for gene sequence homology search.

ii) Analysis of protease inhibitor sequences

The cDNA sequences of EF406275 (putative serpin) and EF406276 (putative BBI) as determined by RACE were analysed by A. Prins using the following online tools: BLASTn and BLASTx at GenBank (Altschul et al., 1997), WU-blastn V2.0 (http://blast.wustl.edu/; Gish, W., 1996-2006) on the EMBL database, ORF finder (http://www.ncbi.nlm.nih.gov/gorf/gorf.html), BLASTx (Gish and States, 1993), ProtParam (Gasteiger et al., 2005), TargetP (http://www.cbs.dtu.dk/services/TargetP/; Emanuelsson et al., 2000), and Eukaryotic Linear Motif Resource (ELM) (http://elm.eu.org/; Puntervoll et al., 2003). After identification of their respective coding

sequences, protein homologs of the putative serpin and putative BBI genes were identified by translated homology search (BLASTx) at GenBank. This algorithm translates the query from nucleotide codons to amino acid sequence and compares this to known protein sequences in the GenBank database. Amino acid sequences were aligned using ClustalW (1.83: http://www.ebi.ac.uk/Tools/clustalw/) (Chenna et al., 2003).

4.3.12 Phylogenetic analysis of putative serpin and BBI sequence

Phylogentic analysis of the putative serpin and putative BBI was performed by P. Verrier (Rothamsted Research). Translated gene sequences were compared to protein homologs by phylogenetic comparison, the alignments being determined by ClustalW (in VectorNTI), and the best unrooted tree was generated with PAUP4* in default parameter configuration and the resultant trees were displayed using the PhyloDraw package.

4.3.13 Analysis of photosynthesis-related transcript abundance

To compare expression of photosynthesis-related transcripts in maize leaves grown in air or with CO_2 enrichment, raw intensity levels of photosynthesis-related probes as detected by microarray analysis were compared. To do this, a keyword search was first done at the NetAffx website to identify all probes on the maize microarray identified under the keywords "RuBisCO", "ribulose", "photosynthesis", and "carbonic anhydrase". The effect of CO_2 enrichment on transcript abundance as detected by microarray study was determined by comparing expression intensity levels of transcripts obtained from leaves grown either with CO_2 enrichment or in air. Difference in expression level was expressed as a percentage for analysis.

4.3.14 Photosynthesis and related parameters

Photosynthesis, transpiration, and stomatal conductance rates were measured on leaves 5-6 and leaves 11-12 of 9 week-old maize plants, using a portable Infra Red Gas Analyser (CIRAS-I; PP systems, UK). The flow rate was 300ml min^{-1}, the CO_2 concentration in the chamber was 350 $\pm$20µl l^{-1} and light intensity was 800µmol m^{-2} s^{-1}.
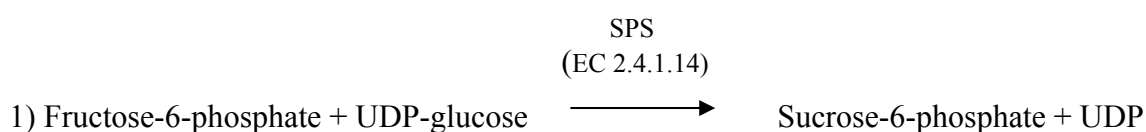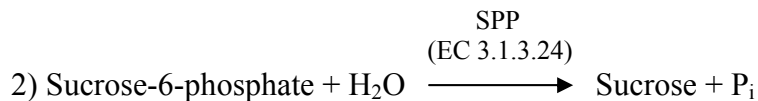
4.3.15   Sugar metabolism enzyme activity

i) Sucrose phosphate synthase

SPS activities were measured in maize leaves according to Guy et al. (1992) with minor changes. Frozen leaf tissue (approximately 0.25g) was crushed in a mortar with liquid nitrogen in extraction buffer (1:20 [w/v]) containing 100mM Tricine (pH7.5), 200mM KCl, 5mM DTT, 5mM $MgCl_2$, 1.3mM EDTA, 4% (w/v) Polyclar AT, and 1% (v/v) protease inhibitor cocktail (Sigma). The homogenates were centrifuged at 15 000rpm for 3min and the supernatants were desalted on a Sephadex G-25 column (PD-10, GE Healthcare) using an elution buffer containing 100mM Tricine (pH 7.5), 200mM KCl, 5mM $MgCl_2$, and 1.3mM EDTA. Samples were diluted 1:1 (v/v) before use. SPS activities were measured under V_{max} conditions in a buffer containing 50mM MOPS-NaOH (pH 7.5), 15mM $MgCl_2$, 1.3mM EDTA, 10mM uridine 5'-diphosphoglucose, 40mM glucose-6-phosphate, and 10mM fructose-6-phosphate (reaction buffer). Desalted, diluted extract (35µl) was incubated with 35µl reaction buffer at 25ºC for 15min before the reaction was terminated by the addition of 70µl NaOH (7.5M). Samples were then incubated in a water bath at 100ºC for 10min and allowed to cool before sucrose content in the solution was measured. To quantify the amount of sucrose formed in the reaction solution, 1mL anthrone reagent (0.14% anthrone in 74% HCl) was added to each reaction tube and incubated at 40ºC for 20min. The absorbance of the solution was then measured at a wavelength of 620nm. Sucrose in the extract produced by SPS activity was calculated from a sucrose standard curve containing 0, 1, 2, 3, 4, 5, 10, or 14µg sucrose in deionised water. For the standard curve, sucrose was dissolved in water (70µl), after which 70µl NaOH (7.5M) was added, and solutions were incubated in a water bath at 100ºC for 10min before adding anthrone reagent as described above. Control reactions were performed using a buffer lacking uridine 5'-diphosphoglucose. Values obtained from control reactions were subtracted from values obtained with samples. Two independent extractions were done for each measurement from tissue pooled from 3 plants, and all measurements were done in duplicate.

The reactions that the sucrose phosphate assay is based on is:

<center>SPS
(EC 2.4.1.14)</center>

1) Fructose-6-phosphate + UDP-glucose $\longrightarrow$ Sucrose-6-phosphate + UDP

$$\text{2) Sucrose-6-phosphate} + H_2O \xrightarrow[\text{(EC 3.1.3.24)}]{\text{SPP}} \text{Sucrose} + P_i$$

Glucose-6-phosphate acts as an activator compound in this reaction since it favours the dephosphorylation of phospho-SPS (less active) to active SPS by SPS protein phosphatase (SPSPP) and also increases catalytic activity *in situ* as a result of allosteric regulation (Huber and Huber, 1992). This assay is a colorimetric method to measures the amount of sucrose formed in reaction 2, since sugars react with the anthrone reagent under acidic conditions to yield a blue-green color. There is a linear relationship between the absorbance and the amount of sugar that is present in the sample. This method determines both reducing and non-reducing sugars because of the presence of the strongly oxidizing sulfuric acid. It is a non-stoichiometric quantification method and therefore it is necessary to prepare a calibration curve using a series of standards of known carbohydrate concentration.

ii) Sucrose synthase

Sucrose synthase activities were measured according to Guy et al. (1992) in desalted extract prepared as for the SPS assay. SuSy activities were measured in the sucrose synthesis direction, using the same buffer as for SPS, except that 10mM fructose replaced the fructose-6-phosphate. Reactions were set up and treated as for SPS in order to measure sucrose in the reaction solution by employing the anthrone method as described above. Control reactions were performed using a buffer lacking uridine 5'-diphosphoglucose. Values obtained from control reactions were subtracted from values obtained with samples. Two independent extractions were done for each measurement from tissue pooled from 3 plants, and all measurements were done in duplicate. The reaction that the sucrose phosphate assay is based on is:

$$\text{3) Fructose} + \text{UDP-glucose} \xrightleftharpoons[]{\substack{\text{SuSy} \\ \text{(EC 2.4.1.13)}}} \text{Sucrose} + \text{UDP}$$
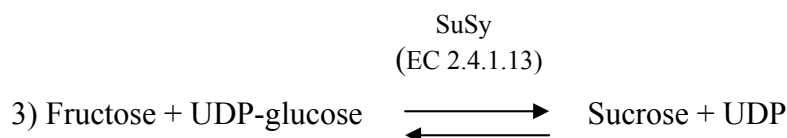
While *in vivo* the sucrose cleavage reaction is favoured (Huber and Huber, 1996; Kruger, 1990), in this assay UDP-glucose is added to the desalted extract, which pushes the balance of the reversible reaction in the direction of sucrose synthesis. The amount of

sucrose formed in reaction 3 is determined colorimetrically through the anthrone method as detailed in section 4.3.16 I).
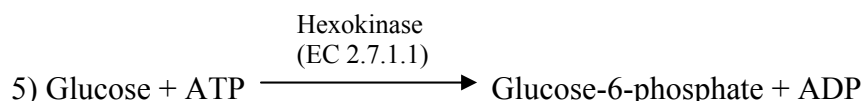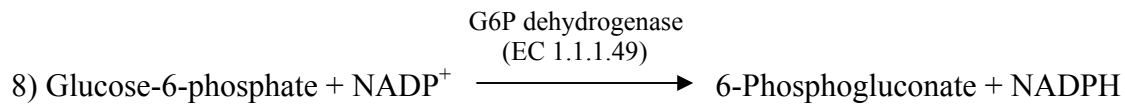
iii) Invertase

Invertase activities were measured in the same desalted extracts as for SPS and SuSy activities. Samples (100μl) were incubated in a 3-fold excess of buffer containing 100mM sodium citrate, 100mM NaH$_2$PO$_4$, and 100mM sucrose at either pH4.8 (to measure acid invertase activity), or pH7.0 (to measure neutral invertase activity) for 2h at 25ºC after which the reaction was stopped by incubating at 100°C for 5min. Two independent extractions were done for each measurement, and all measurements were done in duplicate. For the quantification of acid and neutral invertase activities respectively, 10-20μl and 20-40μl was added to 100μl 2x assay buffer [200mM imidazole, 10mM MgCl$_2$, 3mM ATP, 1mM NADP, 0.04% (w/v) BSA] and made up to a final reaction volume of 200μl with deionised water, in separate wells in a 96-well plate. To measure the amount of hexose formed by hydrolysis of sucrose by invertase (reaction 4), the method of Jones et al. (1977) was followed. Coupling enzymes (0.1U each of hexokinase, phosphoglucose isomerise, and G6P dehydrogenase, Roche, UK) were added to reaction solutions and the resultant production of NADPH was observed as the increase in absorption at 340nm measured on a plate reader (Spectramax, Molecular Devices, UK). The molar extinction coefficient of NADPH (6220 M^{-1} cm^{-1}) at 340nm was used to measure the amount formed, taking into account that a 200μl volume represents a path-length of 0.5cm.

Invertase catalyses the following reaction:

$$\text{4) Sucrose + H}_2\text{O} \xrightarrow[\text{(EC 3.2.1.26)}]{\text{Invertase}} \text{Glucose + Fructose}$$
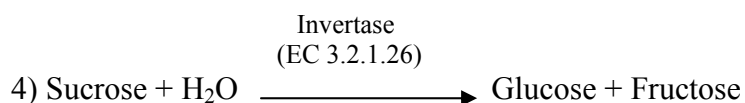
In the reaction solutions incubated with an excess of substrate (sucrose), the sucrose is hydrolysed to glucose and fructose (hexoses) by maize endogenous invertases. Hexose content of samples was measured according to Jones et al (1977) where the addition of the coupling enzymes hexokinase, glucose-6-phosphate dehydrogenase, and phosphoglucose isomerise catalyse the following reactions:

$$\text{5) Glucose + ATP} \xrightarrow[\text{(EC 2.7.1.1)}]{\text{Hexokinase}} \text{Glucose-6-phosphate + ADP}$$

$$\text{6) Fructose + ATP} \xrightarrow[\text{(EC 2.7.1.1)}]{\text{Hexokinase}} \text{Fructose-6-phosphate + ADP}$$

$$\text{7) Fructose-6-phosphate} \xrightarrow[\text{(EC 5.3.1.9)}]{\text{Phosphoglucose isomerase}} \text{Glucose-6-phosphate}$$

$$\text{8) Glucose-6-phosphate + NADP}^+ \xrightarrow[\text{(EC 1.1.1.49)}]{\text{G6P dehydrogenase}} \text{6-Phosphogluconate + NADPH}$$
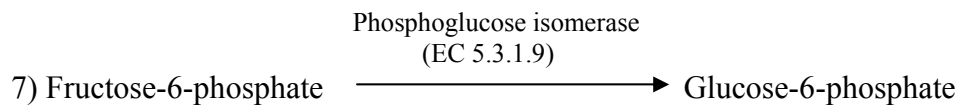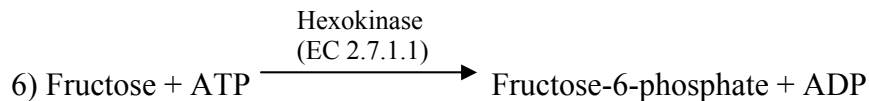
For this assay, a mixture of all three coupling enzymes was added to the reaction solution in order to catalyze reactions 5-8 concurrently. For the quantification of acid and neutral invertase activities in extract, 10-20µl and 20-40µl was respectively added to a final volume of 200µl in a 96-well plate. After addition of coupling enzymes to this solution, the resultant production of NADPH was observed as the increase in absorption at 340nm. The molar extinction coefficient of NADPH (6220 M^{-1} cm^{-1}) at 340nm was used to measure the amount formed, taking into account that a 200µl volume represents a path-length of 0.5cm. Therefore, since in a 1cm path length 1AU = 1/6.22 µM, it can be calculated that in a 200µl volume (0.5cm path length) NADPH formed (µmol) = ΔA_{340}/6.22x0.5. Since one molecule NADPH is formed for each molecule hexose, the amount of hexose is directly equivalent to the amount of NADPH.

4.3.16   Statistical methods

The gas exchange data was analyzed by ANOVA. Data for all other physiological parameters was analyzed by Student's t-test. Correlation analysis between transcript abundance and hexose and sucrose content of leaves was done with the Statistica software (v 7.1; StatSoft Inc).

4.4   Results

4.4.1   High CO_2 effects on whole plant morphology and photosynthesis

Maize plants were grown eight weeks in either air (350µl l^{-1} CO_2) or with CO_2 enrichment (700µl l^{-1} CO_2) (Fig. 4.6 A). The anthers were present at this growth stage and cobs were starting to form. Hence, all the leaves can be classed as source leaves at this growth stage.
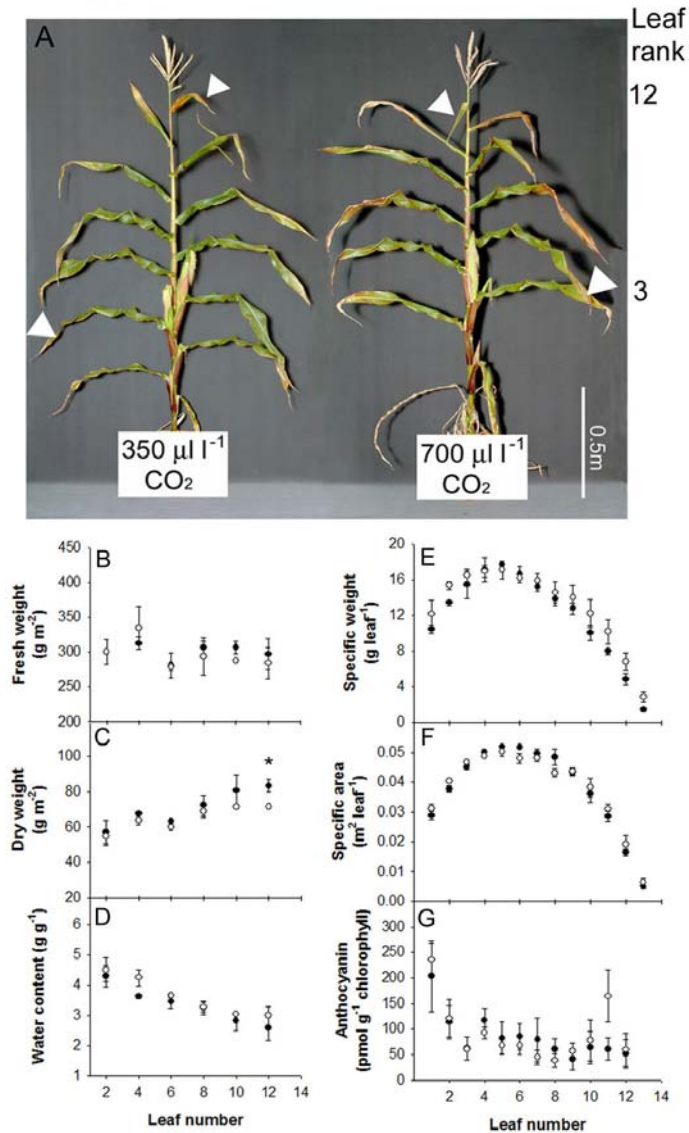
Figure 4.6. The growth CO_2 phenoytpe in maize. Maize phenotype at the point of harvest and analysis (A). Arrows indicate leaf ranks sampled for trancriptome analysis. Leaves harvested from air-grown plants (closed circle) or plants grown with CO_2 enrichment (open circle) were analysed for fresh weight (B) and dry weight (C) values that were used to calculate tissue water content (D); Specific leaf weight (E); Specific leaf area (F); leaf anthocyanin content (G). Significant differences at $P < 0.05$ indicated by the symbol (*).

All the leaves had high rates of photosynthesis regardless of the position of the stem (Table 4.4). However, values obtained for the oldest mature leaves i.e. leaf ranks 3-5, were significantly lower than those measured in leaf rank 12, suggesting that these leaves were only in the early stages of senescence. The development-dependent decreases in CO_2 assimilation rates were of the same order (29-31%) in both air and high CO_2 –grown plants (Table 4.4). While no significant decreases in photosynthetic CO_2 assimilation rates

(expressed on a surface area basis) resulted from growth with CO_2 enrichment, transpiration rates were significantly decreased in the high CO_2 –grown plants (Table 4.4).

Table 4.4 Acclimation of photosynthesis, transpiration, and stomatal conductance to CO_2 enrichment in young source leaves (leaf rank 12) and old source leaves (leaf rank 5) of 8 week-old plants. Values represent mean ± SE; n=4.

CO_2 ($\mu l \ l^{-1}$)	Leaf rank	Photosynthesis ($\mu mol \ m^{-2} \ s^{-1}$)	Transpiration ($mmol \ m^{-2} \ s^{-1}$)	Stomatal conductance ($mmol \ m^{-2} \ s^{-1}$)
350	12	20.96 ± 1.50	3.10 ± 0.37	119.0 ± 15.8
350	5	14.48 ± 0.25	2.69 ± 0.14	101.25 ± 8.9
700	12	17.28 ± 2.93	2.95 ± 0.42	83.48 ± 13.8
700	5	12.24 ± 2.24	2.14 ± 0.31	58.6 ± 2.2

ANOVA analysis:
Significant difference at $P < 0.05$ indicated by *

Parameter	Leaf Rank	CO_2 level	Interaction
Photosynthesis	0.014*	0.163	no
Transpiration	0.087	0.305	no
Stomatal conductance	0.105	0.007*	no

No differences in phenotype were observed between air and high CO_2–grown plants at this stage (Fig. 4.6 A). There were no significant differences in the fresh weights (Fig. 4.6 B), the dry weights (Fig. 4.6 C), or tissue water contents (Fig. 4.6 D) of leaves at equivalent positions on the stem. The leaf fresh weight values were similar regardless of ontogeny, but the dry weight values were greatest in the young leaves and decreased with leaf position on the stem (1 to 12). The oldest source leaves had the lowest dry weight values (Fig. 4.6 C). Similarly, the tissue water content was greatest in oldest source leaves and decreased gradually with the leaf position on the stem, the young leaves having the lowest tissue water contents (Fig. 4.6 D). The leaves were at their maximum size and weight at leaf rank 5 (Fig. 4.6 E and 4.6 F) regardless of whether the plants had been grown in air or with CO_2 enrichment. The total anthocyanin contents, which have been taken as an indicator of stress, increased progressively as the leaves aged being highest in leaf rank 1, but values were similar in plants grown in air or with CO_2 enrichment (Fig. 4.6 G).

4.4.2   CO$_2$ –dependent effects on the leaf transcriptome

The transcriptome of leaf ranks 3 and 12 was compared in air-grown and high CO$_2$-grown plants (Web Table 1-7; PDF files on CD). Leaf developmental stage/ontogeny had a much greater effect on the leaf transcriptome than growth CO$_2$ level (Fig. 4.7 A and B).
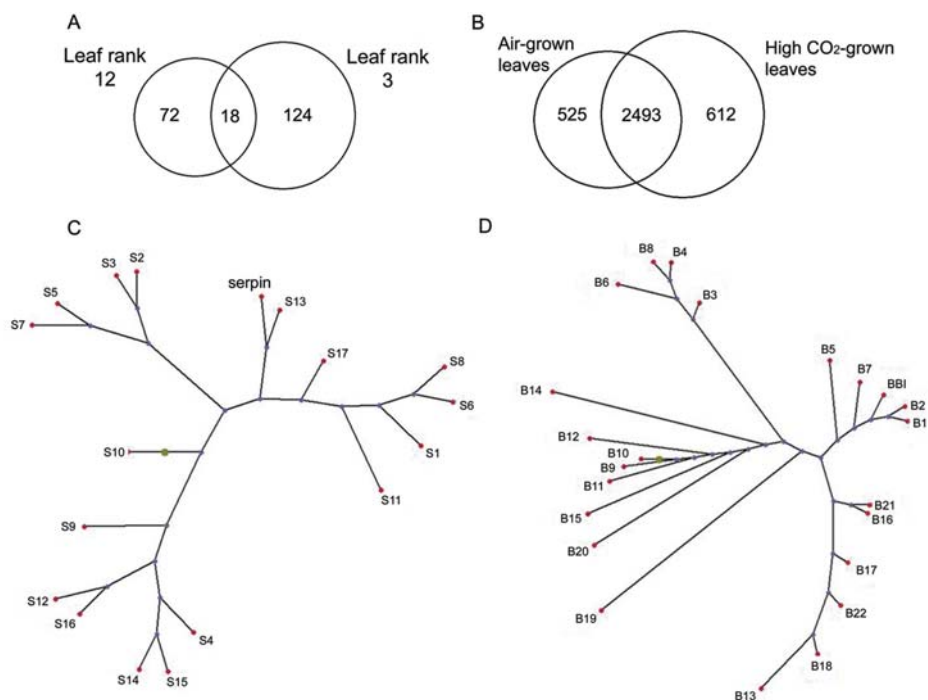
Figure 4.7 Transcriptome analysis of young and old source leaves from air-grown plants or plants grown with CO$_2$ enrichment. Comparisons of the numbers of CO$_2$ enrichment-modulated transcripts at the different leaf ranks (A) and the numbers of transcripts that were differentially expressed as a result of leaf position on the stem (B). Phylogenetic trees showing the relationships between putative serpin and known serine protease inhibitor protein sequences (S1-S17; C) and putative BBI and known Bowman-Birk serine protease inhibitor protein sequences (B1-B22, D).

Table 4.5 Sequences used in phylogenetic analysis (Fig. 4.7 C and D).

Sequence	Accession	Definition	Sequence	Accession	Definition
serpin	EF406275.1	Zea mays putative serine type endopeptidase inhibitor	BBI	EF406276.1	Zea mays putative Bowman-Birk serine protease inhibitor
S1	Q43502	Protease inhibitor type-2 CEVI57 precursor	B1	ABL63911.1	Bowman-Birk serine protease inhibitor [Musa acuminata]
S2	AAF18450.1	Protease inhibitor type II precursor NGPI-1 [Nicotiana glutinosa]	B2	P81713	Bowman-Birk type trypsin inhibitor (WTI)
S3	AAF18451.1	Protease inhibitor type II precursor NGPI-2 [Nicotiana glutinosa]	B3	AAO89510.1	Bowman-Birk protease inhibitor [Glycine microphylla]
S4	ABA42892.1	Trypsin protease inhibitor precursor [Nicotiana benthamiana]	B4	BAB86783.1	Bowman-Birk type protease isoinhibitor A1 [Glycine soja]
S5	ABA42904.1	Trypsin protease inhibitor precursor [Nicotiana acuminata]	B5	P16343	Bowman-Birk type protease inhibitor DE-4 (DE4)
S6	AAL54921.2	Protease inhibitor IIb [Solanum americanum]	B6	BAB86784.1	Bowman-Birk type protease isoinhibitor A2 [Glycine soja]
S7	AAR84197.1	Putative 6 repeat protease inhibitor [Nicotiana attenuata]	B7	P82469	Bowman-Birk type protease inhibitor 1
S8	AAR37362.1	Protease inhibitor 2b precursor [Solanum nigrum]	B8	P01055	Bowman-Birk type protease inhibitor precursor (BBI)
S9	AAQ56588.1	6-domain trypsin inhibitor precursor [Nicotiana attenuata]	B9	P81484	Bowman-Birk type protease inhibitor PVI-3(2)
S10	AAO85558.1	7-domain trypsin inhibitor precursor [Nicotiana attenuata]	B10	P81483	Bowman-Birk type protease inhibitor PVI-4
S11	Q40561	Protease inhibitor type-2 precursor	B11	CAD32699.1	double-headed trypsin inhibitor [Phaseolus vulgaris]
S12	ABA86556.1	Six domain protease inhibitor [Nicotiana tabacum]	B12	CAD32698.1	double-headed trypsin inhibitor [Phaseolus vulgaris]
S13	BAA95792.1	Protease inhibitor II [Nicotiana tabacum]	B13	S09415	protease inhibitor - cowpea
S14	AAZ20771.1	Insect injury-induced protease inhibitor [Nicotiana tabacum]	B14	Q9S9E3	Horsegram inhibitor 1
S15	AAF14181.1	Protease inhibitor precursor [Nicotiana alata]	B15	CAL69237.1	double-headed trypsin inhibitor [Phaseolus parvulus]
S16	AAA17739.1	Protease inhibitor precursor	B16	ABD91575.1	trypsin inhibitor [Vigna radiata var. sublobata]
S17	P01080	Protease inhibitor type-2 K precursor	B17	AAW84292.1	trypsin inhibitor [Lens culinaris]
			B18	AAO43982.1	trypsin inhibitor [Vigna unguiculata subsp. sesquipedalis]
			B19	P01059	Bowman-Birk type protease inhibitor DE-4
			B20	P01056	Bowman-Birk type protease inhibitor
			B21	ABD91574.1	trypsin inhibitor [Vigna trilobata]
			B22	CAC81081.1	trypsin inhibitor [Vigna unguiculata]

Growth with CO_2 enrichment resulted in the differential expression of only 90 transcripts (Web Table 1) in the young (leaf 12) source leaves, while 142 transcripts were differentially expressed in the old (leaf 3) source leaves (Web Table 2). The high CO_2 signature of young source leaves (leaf 12) included transcripts involved in carbohydrate and amino acid metabolism (Web Table 1). Putative ADPglucose pyrophosphorylase and starch synthase transcripts were significantly higher in the young source leaves in air compared to high CO_2. Similarly, putative glutamine synthetase, aspargine synthetase and tryptophan synthase transcripts were significantly higher in leaf 12 in air compared to high CO_2. In contrast, while the older leaves lacked high CO_2–dependent effects on these transcripts, they showed a marked decrease in the abundance of nitrate reductase and methionine synthase transcripts at high CO_2.

Relatively few photosynthesis-related sequences were significantly affected by CO_2 enrichment at the chosen cut off point in this study (above the 50% level). To detect any possible CO_2 enrichment-dependent effects on transcripts associated with photosynthesis, the cut-off point for significance was decreased to 10% (Web Table 3). At this level, carbonic anhydrase transcripts were decreased and phosphoenolpyruvate carboxylase and phytase transcripts were increased by CO_2 enrichment. RuBisCO large subunit expression was not significantly affected by the growth CO_2 level, showing air/CO_2 enrichment ratios of 1.00 in young source leaves and 0.97 in old source leaves, respectively. However, RuBisCO SSU transcripts were increased more in air than in high CO_2, an effect that was greatest in the young source leaves. A RuBisCO activase precursor transcript was slightly increased in the older source leaves compared to those grown in air.

While the expression of chlorophyll a/b-binding proteins CP29 (Lhcb4) and CP26 (Lhcb5) was unaffected by CO_2 enrichment, transcripts encoding CP24 (Lhcb6) and a magnesium chelatase subunit I precursor, which plays a role in chlorophyll biosynthesis, were induced in young source leaves grown in air compared to those with CO_2 enrichment. In addition, transcripts encoding PGR5, which has been linked to ferredoxin:plastoquinone oxidoreductase-mediated cyclic electron flow and ferredoxin transcripts were induced more in the old source leaves than the young leaves in air compared to similar leaves grown with CO_2 enrichment.

In contrast to the transcripts associated with photosynthesis that showed relatively minor CO_2 enrichment-dependent effects, all of the following transcripts were significantly affected by high CO_2 above the 50% threshold. While several transcripts involving signaling, DNA-binding and the cell cycle including a putative ethylene responsive element binding factor were differentially expressed as a result of growth with CO_2 enrichment, the most noticeable changes were in transcripts involved in cell rescue and defense responses and in secondary metabolism, which were differentially modified in plants grown in air (Web Tables 1 and 2). In particular, the abundance of ACC oxidase transcripts was higher in both young and old source leaves in air compared to high CO_2 suggesting that the capacity for ethylene production is decreased at high CO_2. Relatively few antioxidant defense transcripts were differentially regulated in response to CO_2 enrichment. Of these, it is notable that *cat*1 transcripts were higher in air than with CO_2 enrichment, but this was restricted to the young source leaves. In contrast, three glutathione S-transferases and three putative peroxidase transcripts were highly expressed in air in the older but not the young source leaves. Hemoglobin (HB2) transcripts were significantly increased in air in both young and old source leaves. Similarly, a number of chitinase and glucanase transcripts were increased in air compared to CO_2 enrichment, in either or both young and old source leaves. Two maize heat shock proteins (HSP22 and HSP26) were much lower in the young and old source leaves in air than with CO_2 enrichment (Web Tables 1 and 2).

Eighteen high CO_2–modulated transcripts were identical (based on probe identity) in leaf ranks 3 and 12 (Table 4.6). Of these, pathogenesis-related protein 10 and two putative peroxidases were decreased in young source leaves but increased in the old source leaves (Table 4.6). The 18S and 23S ribosomal subunit transcripts were decreased in air-grown leaves. Of the ten transcripts that are more abundant in air-grown young and old source leaves, two sequences that were identified as a putative serine protease inhibitor and a putative Bowman-Birk (BBI) serine protease inhibitor were selected for further analysis as they are associated with protein turnover and stress response, which was of major interest in this study.

these transcripts were designed using the Primer Express software (v2.0, Applied Biosystems, UK) and synthesised by Sigma Genosys (Sigma, UK) (Table 2.2). Ubiquitin (MUB3; Zm.12132.3.S1_a_at), thioredoxin M (Zm.719.1.A1_at), and cyclophilin (Cyp; AFFX-Zm_Cyph_3_at) were selected as endogenous controls based on similar microarray expression values higher than 10 000 (Table 4.2).

Table 4.1. Probe sets used to design primers for qPCR, expression levels and primer sequences.

Probe set used for primer design	Maize gene title or description	Log$_2$ (air / high CO$_2$)		Forward primer	Reverse primer
		Young leaves	Old leaves		
Zm.3332.1.A1_at	putative serpin	0.541	0.728	TCGATCTGGACAAA GACCAACC	ACAGGCGCCAAAGT TTTA
Zm.4270.2.A1_a_at	putative BBI	1.919	0.622	AGTGCCAGTGCAAT GACGTGT	AATTCCTGCACCGA CCTTGAC
		Log$_2$ (young / senescent)			
		Air	High CO$_2$		
Zm.13430.1.S1_at	Cell wall invertase Incw4	0.625	0.805	GAGGAGCACGAGA CCATCAATT	TCCACCACCGAGTG ATCAATC
Zm.231.1.S1_at	Invertase	-0.575	-0.626	ATACAACCACGACT ACATGGCG	GCATTGCATCGATC AGATGTCT
Zm.3478.1.S1_a_at	sucrose synthase 3	0.800	0.968	TTCTGGAAGTACGT GTCGAAGC	CTCAAGGTAGCGCC TCGTCT
Zm.6977.1.S1_at	sucrose synthase (EC 2.4.1.13)	-1.220	-1.209	TGAAGTACCGTAGC CTGGCAA	CGTACTAATCGAAG GACAGCGG
Zm.6977.5.S1_a_at	sucrose synthase (EC 2.4.1.13)	-1.031	-0.990	-	-
Zm.26.1.A1_at	sucrose phosphate synthase	1.109	1.453	TTCCAGCGGCATGT GAATTT	ATACACACCCGCGG TACTGTTC

Table 4.6 CO_2-modulated transcripts in leaf rank 3 (Young leaves) and 12 (Old leaves)

Probe ID	Genbank accession of probe target	Log$_2$ (air / high CO$_2$) Young leaves	Old leaves	Maize gene name or function	Best BLASTx hit accession	Protein description	% identity	e-value	bitscore
Zm.11586.1.A1_at	BM379136	0.844	0.561	Transcribed locus	no hit	-	-	-	-
Zm.11985.1.A1_at	CF636772	0.783	0.608	Hb2: Hemoglobin 2 (Hb2)	NP_179204.1	AHB1 [A. thaliana]	67.5	6E-11	63.5
Zm.1419.1.S1_at	CO527884	1.393	0.548	PCO072275 mRNA sequence	NP_914960.1	putative dermal glycoprotein precursor [O. sativa]	55.96	5E-29	124
Zm.1595.1.S1_at	CD967190	1.890	0.918	PCO155066 mRNA sequence	NP_191010.1	ATEP3; chitinase [A. thaliana]	67.86	5E-28	120
Zm.3332.1.A1_at	**BM379802**	**0.541**	**0.728**	**PCO129929 mRNA sequence**	**NP_177351.1**	**serine-type endopeptidase inhibitor [A. thaliana]**	**68**	**8E-18**	**86.3**
Zm.4270.2.A1_a_at	**CF628998**	**1.919**	**0.622**	**PCO107455 mRNA sequence**	**NP_910046.1**	**putative Bowman-Birk serine protease inhibitor [O. sativa]**	**48**	**6E-16**	**80.1**
Zm.6689.1.A1_at	BM381797	0.991	0.807	Transcribed locus, weakly similar to XP_463709.1 putative glucan endo-1,3-beta-D-glucosidase [O. sativa]	NP_914603.1	putative beta 1,3-glucanase [O. sativa]	82.35	1E-36	149
Zm.6689.1.A1_s_at	BM381797	0.707	0.634	Transcribed locus, weakly similar to XP_463709.1 putative glucan endo-1,3-beta-D-glucosidase [O. sativa]	NP_914603.1	putative beta 1,3-glucanase [O. sativa]	82.35	1E-36	87
Zm.8130.1.A1_at	CK369071	0.735	0.579	Transcribed locus, moderately similar to XP_467491.1 unknown protein [O. sativa]	no hit	-	-	-	-
ZmAffx.1198.1.A1_at	BE056195	1.273	1.047	CL3918_1 mRNA sequence	XP_469149.1	putative antifungal zeamatin-like protein [O. sativa]	77.5	1E-14	75.9
Zm.4510.1.A1_a_at	CF636202	0.555	-0.606	PCO135232 mRNA sequence	no hit	-	-	-	-
Zm.17997.1.A1_at	CK369019	-0.658	0.712	PCO129777 mRNA sequence	NP_917067.1	putative phosphoethanolamine N-methyltransferase [O. sativa]	84.26	2E-49	192
Zm.1967.1.A1_at	BG836522	-0.681	0.892	PCO091453 mRNA sequence	Q29SB6	pathogenesis-related protein 10. [Z. mays]	97.81	3E-68	251
Zm.2707.1.S1_at	BG842199	-0.558	1.276	PCO104850 mRNA sequence	XP_479513.1	peroxidase [O. sativa]	81.08	7E-41	164
Zm.3630.1.A1_at	BM380179	-2.577	1.078	Transcribed locus, strongly similar to XP_473863.1 OSJNBa0070C17.11 [O. sativa]	XP_550375.1	putative proline rich protein [O. sativa]	60.71	4E-26	115
Zm.369.1.A1_at	AF035460.1	-0.873	-0.599	Zea mays low molecular weight heat shock protein precursor (hsp22)	XP_467890.1	putative low molecular weight heat shock protein [O. sativa]	89.04	8E-23	103
ZmAffx.1215.1.S1_s_at	6273844	-0.505	-0.585	Zea mays 18S small subunit ribosomal RNA gene	XP_466329.1	18S small subunit ribosomal RNA	38.460	0.980	29.6
ZmAffx.1221.1.S1_at	11990232-113	-1.113	-1.223	Zea mays 23S rRNA	YP_358637.1	23S ribosomal RNA	92.680	0.000	88.6

4.4.3 Characterization of two CO_2 –modulated serine protease inhibitors

The full-length gene sequences of these inhibitors were obtained by RACE and compared to those of known similar inhibitors in the databases (Fig. 4.8). The putative serine protease inhibitor EF406275 (serpin) is 48% homologous to an *Arabidopsis* serine-type endopeptidase inhibitor (NP_177351.1; bit score 86.3; E=6e-16) that aligns to the *Arabidopsis* protein in the +2 frame (Fig. 4.8 A). The putative Bowman-Birk inhibitor (BBI) sequence has a 68% sequence similarity to a patented maize sequence, which is described as a maize protease inhibitor-like polynucleotide (AR494954; patent number US6720480-A/1, 13-APR-2004) (Fig. 4.8 B).

```
A  Serpin        MAASKFYVASCALL--LIGVVLLGQQGIDGAVACPQFCLDVDYVTCPSSGSEKLPARCNC 58
   NP_177351.1   MVTYKIWVMSFIIAGAILGGIIPGVTTTKTAIACPLYCLQVEYMTCPSSGADKLPPRCNC 60
                 *.: *::* *  :    ::* :: *    . *:*** :**:*:*:******:;***.****

   Serpin        CMTPKGCTLHLSDGTQQTCS- 78
   NP_177351.1   CLAPKNCTLHLSDSTTIHCSK 81
                 *:;**.*******.*   **

B  BBI           MRP-----QLILVGTLAVLAILAALGEGSS-------------------------SWP 28
   ABL63911.1    MRYNMVVFSLVLMVAAAFFASATTTASSSHPELRSALSTKGHEEDGEGVGERSRQRRTWP 60
                 **       .*:*: : *.:*  :: ...*                           :**

   BBI           CCNNCGACNKKQPPECQCNDVSVNGCHPECMNCVKVGAGIRPGMGHGPVVTYRCDDVLTN 88
   ABL63911.1    CCDRCGGCTKSTPPQCQCQDMVRS-CHPSCRHCVRSPLSVSP-------PLYQCMDRIPN 112
                 **:.**.*.*. **:***:*:   . ***.* :**:   .: *        *:* * :.*

   BBI           FCQSSCPEAPAP-- 100
   ABL63911.1    YCRRRCTPEPLLAQ 126
                 :*:  *.  *
```

Consensus symbols:
* all residues in the column are identical in all sequences in the alignment
: conserved substitutions are observed
. semi-conseved substitutions are observed

Figure 4.8 Pairwise alignments of two putative serine protease inhibitor protein sequences affected by CO_2 enrichment. The putative serpin is aligned with the closest protein homolog (NP177351.1; A) and the putative BBI is also aligned with the closest protein homolog (ABL6391.1; B).

Analysis of the putative serine protease inhibitor with the Eukaryotic Linear Motif Resource (ELM) (http://elm.eu.org) revealed the presence of a potato type II protease inhibitor (pin2) domain from residue 29 to 73 (Fig. 4.9). Members of the pin2 family are protease inhibitors that contain eight cysteines that form four disulphide bridges, and that inhibit serine proteases. Eight such cysteine residues were identified in the putative serpin (Fig. 4.9). A potential signal peptide was also identified from residue 1 to 28 consistent with other pin2 inhibitors (Barta et al., 2002).

```
                        1 ↓↓2         3            4 56    7           8
Maize_putserpin   -VACPQFCLD-VDYVTCPSSGSEKLPARCNCCMTP-KGCTLHLSDGTQQTCS 49
Maize_pin2        -VACPQFCLD-VDYVTCPSSGSEKLPERCNCCMTP-KGCTLHLSDGTQQTC- 48
Sorghum_pin2      AVPCPQYCLE-VDYVTCPSSGSEKLPARCNCCLAP-KGCTLHLSDGTQQTC- 49
Rice_pin2         -KFCPQFCYDGLEYMTCPSTG-QHLKPACNCCIAGEKGCVLYLNNGOVINC- 49
                  ***:*  : ::*:****:*  ::*    ****::  ***.*:*.:*    .*
```

Figure 4.9 Pairwise alignment of the putative serpin (Maize_putserpin) with three serpin sequences identified in maize (Maize_pin2; accession AI947362), sorghum (Sorghum_pin2; accession AI724716), and rice (Rice_pin2; accession AU163886). Conserved cysteine residues that participate in disulphide bridges are in bold and numbered. Arrows indicate the putative protease-contact residues (Barta et al, 2002). Consensus symbols are as in Fig. 4.8.

Analysis of the putative BBI revealed the presence of conserved cysteine residues characteristic of those present in Bowman-Birk inhibitors (Mello et al., 2003). These residues were identified at the 9 conserved positions in the two putative reactive sites of the putative maize BBI. The first two conserved cysteine residues (C1 and C2) were identified at residue 29 in the putative protein when compared to known sequences (Fig. 4.10; Mello et al., 2003).

```
                      12 3  4 ↓      5 6      7  8 9   ↓
Maize_putBBI      SWPCCNNCGACNKKQPPECQCNDVSVNGCHPECMNCVKVGAGIRPG 46
Maize_WIP_P31862  --KCCTNC---NFSFSGLYTCDDVKKD-CDPVCKKCVVAVHASY-- 38
Suc_AY093810      SWPCCDNCGACNKKFPPECQCQDISARGCHPECKKCVKIGGGIPPG 46
Suc_AY093809      SWPCCDNCGVCNKKFPPDCQCSDVSVHGCHPECKKCVKQGAGIPPG 46
                  ** **   *  .  .    *.*:.   *.* * :**      .
```

Figure 4.10 Pairwise alignment of the putative BBI (Maize_putBBI), two BBI sequences identified in *S. officinarum* (Suc_AY093810 and Suc_AY093809), and a wound-induced protein from maize (Maize_WIP_P31862). Conserved cysteine residues that participate in disulphide bridges are in bold and numbered. Arrows indicate the putative reactive binding sites (Mello et al, 2003). Consensus symbols are as in Fig. 4.8.

4.4.4 Development-related effects on the transcriptome of source leaves in air and high CO_2-grown plants

In air-grown plants, 3018 transcripts were differentially expressed between young and old source leaves (Web Table 4), while 3105 transcripts showed differential expression between leaf 12 and leaf 3 on plants grown with CO_2 enrichment (Web Table 5). A comparison of the leaf 12 and leaf 3 transcriptomes in air (Web Table 4) and high CO_2 (Web Table 5) revealed that 2493 transcripts were common based on probe set identity (Fig. 4.7 B). Of the transcripts specifically affected by leaf ontogeny/development irrespective of the CO_2 enrichment (Web Table 6), 1336 transcripts were up-regulated and

1157 transcripts were down-regulated in young compared to old source leaves. Transcripts that could not be identified by translated homology search were assigned as "unknown" and totaled 953 sequences. The remaining transcripts were assigned to the 15 functional categories as previously. For the purposes of the present description and discussion we will focus on transcripts in only three categories that are of interest in relation to the focus of this study: carbon metabolism, redox metabolism and protein turnover. However, it is important to note that transcripts associated with storage proteins were only up-regulated in young leaves. Conversely, transcripts associated with vesicle trafficking, signaling, and transposons were decreased in young rather than old source leaves. Sixteen of the 17 transposon-related transcripts that were identified in this study were lower in abundance in the young source leaves.

Re-adjustments in cellular redox metabolism were observed in response to leaf rank (Web Tables 4 and 5). However, there were no clear trends with regard to indications of enhanced oxidation in either young or old source leaves. For examples, while ascorbate oxidase, dehydroascorbate reductase and three putative peroxidases were lower in the older source leaves, monodehydroascorbate reductase, an NADH dehydrogenase and three other peroxidases were enhanced in the older leaves. A number of sequences involved peroxisomal metabolism were modulated by leaf development. Peroxisomal biogenesis factor 11 and catalase 1 transcripts were increased in the old source leaves whereas catalase 2 transcripts were decreased. Similarly, transcripts encoding four ferredoxins, a thioredoxin m, a glutathione (thioredoxin) peroxidase and three rubredoxins were decreased whereas another glutathione (thioredoxin) peroxidase, a ferredoxin-NADP reductase and two protein disulphide isomerases were increased in the old source leaves. A total of 16 glutathione S-transferases were differentially modulated by leaf development with four more abundant in young leaves and twelve predominating in the older leaves.

A distinct differential orchestration of carbohydrate metabolism transcripts was observed between the young and old source leaves with transcripts encoding ribose-5-phosphate isomerise, fructose bisphosphatase, fructose bisphosphate aldolase, triose phosphate isomerise, phosphoglucomutase, UDP-glucose pyrophosphorylase, glyceraldehyde 3-phosphate dehydrogenase, malate dehydrogense, a glucose 6-phosphate dehydrogenase, UDP-glucosyl transferase, beta glucosidase, glucan 1,3-beta glucosidase, ADP-glucose pyrophosphorylase, sucose phosphate synthase, sucose phosphorylase, predominating in

the younger leaves, together with sucrose and other sugar transporters and glucose 6-phosphate transporter, which were much higher in the younger than the older source leaves. Similarly, transcripts encoding starch metabolism enzymes such as beta amylase, phosphorylase, starch synthase and starch branching enzyme were highest in the young source leaves. While transcripts encoding trehalose 6-phosphatase were highest in young source leaves in both air and high CO_2 transcripts encoding trehalose 6-phosphate synthase were only higher in the young source leaves in air. While sucrose synthase 3 was predominant in young source leaves a different sucrose synthase sequence predominated in the older source leaves. Similarly, neutral invertase and a cell wall invertase (incw4) were highest in the young source leaves; transcripts encoding acid invertase were highest in the old source leaves. Transcripts encoding the glucose 6-P/Pi transporter, several glycosyl transferases, beta-fructofuranosidase, mannosidase, a fructose bisphosphate aldolase, a glucose 6-phosphate dehydrogenase were also highest in the oldest leaves, which tended to be richer in transcripts associated with sugar/carbohydrate signaling than the younger source leaves. These included snf7, SNF-1 related protein kinase, SnRK1-interacting protein 1 and hexokinase (Table 4.7). Hexokinase-catalysed phosphorylation of glucose is essential for the repression of photosynthesis-related genes (Moore et al., 2003).

Table 4.7 Abundance of hexokinase transcripts in young mature leaves (rank 12) and old mature leaves (rank 3) compared as a log_2 ratio in leaves grown at 350µl l^{-1} CO_2 or 700µl l^{-1} CO_2.

Probe ID	Description	log_2 (rank 12/rank3)	
		350 µl l^{-1}	700 µl l^{-1}
Zm.5206.1.S1_x_at	Hexokinase	-0.571	-
Zm.5206.2.S1_a_at	Hexokinase	-0.710	-0.512
Zm.5206.3.A1_a_at	Hexokinase	-0.799	-0.525
Zm.8365.1.A1_at	putative hexokinase 1	-	-0.608

With regard to protein turnover, a large number of proteases (36 transcripts), protease inhibitors (11 transcripts), and proteolysis-related sequences (28 transcripts) were differentially expressed as a result of leaf development/ontogeny (Web Table 7). However, CO_2 enrichment had no significant effects on the abundance of these transcripts. Amongst the protease transcripts, eighteen were higher in young compared to old source leaves, and a further eighteen were higher in old compared to young source leaves. Seven of the eleven protease inhibitor sequences were enhanced and four were decreased in young compared to old source leaves. Other related transcripts particularly those involved

in the ubiquitin-proteosome were mainly lower (25 transcripts out of 28) in young than old source leaves.

4.4.5 The effect of leaf position on the response to growth CO_2 levels for the serpin and BBI inhibitor transcripts and transcripts associated with sugar metabolism

To investigate the relationships between effects of growth CO_2 and leaf development on the abundance of transcripts encoding the two putative serine protease inhibitors identified as CO_2–modulated in both young and old source leaves, qPCR analysis of these transcripts on all the leaves on the stem was conducted. For comparison, the abundance of the four invertase and sucrose synthase sequences associated with carbohydrate metabolism identified in the transcriptome analysis as differentially modulated by development were also analysed. These were cell wall invertase, acid invertase, sucrose synthase 3, sucrose synthase, and sucrose phosphate synthase. The abundance of the putative serpin transcripts in air varied according to the position of the leaves and the highest levels were measured in the leaves 1-3 (Fig. 4.11 A). In contrast, no clear trend in putative BBI transcript abundance could be detected at any positions on the stem (Fig. 4.11 B). However, the response of both the putative serpin and BBI transcripts to growth with CO_2 enrichment was dependant on the position of the leaf on the stem (Fig. 4.11 A and B). While putative serpin transcripts were increased as a result of growth with CO_2 enrichment only in the youngest source leaves (Fig. 4.11 A), putative BBI transcripts showed a marked increase in abundance only in the oldest source leaves in response to high CO_2 (Fig. 4.11 B). Growth with CO_2 enrichment had no effect on the abundance of any of transcripts associated with sugar metabolism that were measured (Fig. 4.11 C-G), except for invertase (Fig. 4.11 C). While the abundance of the sugar-associated transcripts varied with the position on the stem the only clear effect of leaf position was observed with SPS transcripts (Fig. 4.11 G), the abundance of which was highest in the young source leaves and decreased progressively in the leaf ranks down the stem and reaching a lowest expression level in the oldest source leaves.
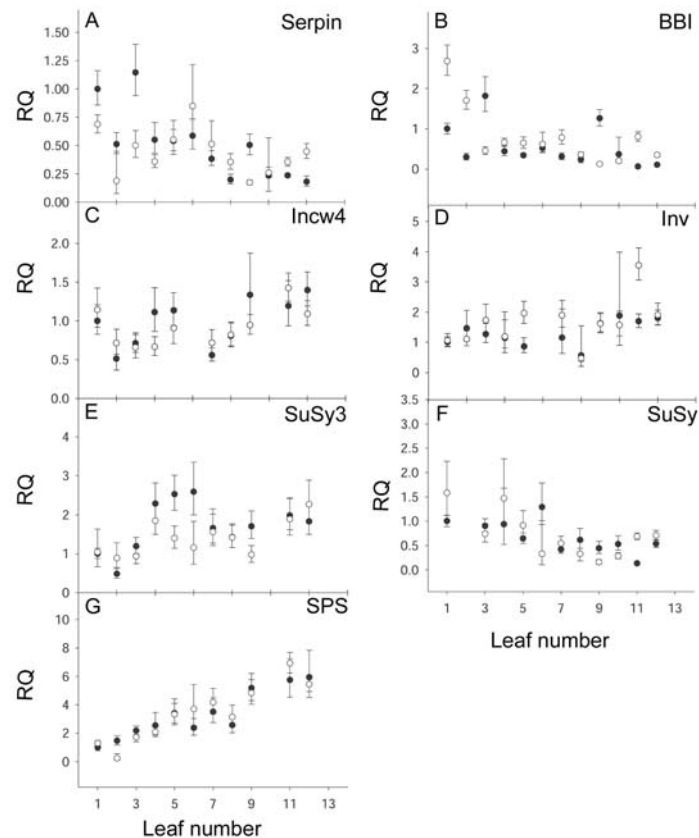
Figure 4.11 Effects of CO_2 enrichment on the abundance of transcripts encoding the two putative serine protease inhibitors and selected transcripts encoding enzymes of sugar metabolism in young and old source leaves. The abundance of transcripts encoding putative seprin (A) putative BBI (B) cell wall invertase (C), invertase (D), sucrose synthase 3 (E), sucrose synthase (F), and sucrose phosphate synthase (G) were determined in all the leaves of air-grown plants (closed circles) or plants grown with CO_2 enrichment (open circles). Values ± max/min were normalised to leaf 1 grown in air (relative quantity, RQ = 1) and expressed relative to thioredoxin transcripts, which were used as the endogenous control.

4.4.6 The effect of leaf position on the response to growth CO_2 levels for tissue carbohydrate contents and invertase and sucrose phosphate synthase activities

The amounts of glucose, fructose, sucrose and starch were measured in all the leaves on the stem (Fig. 4.12 A-D).
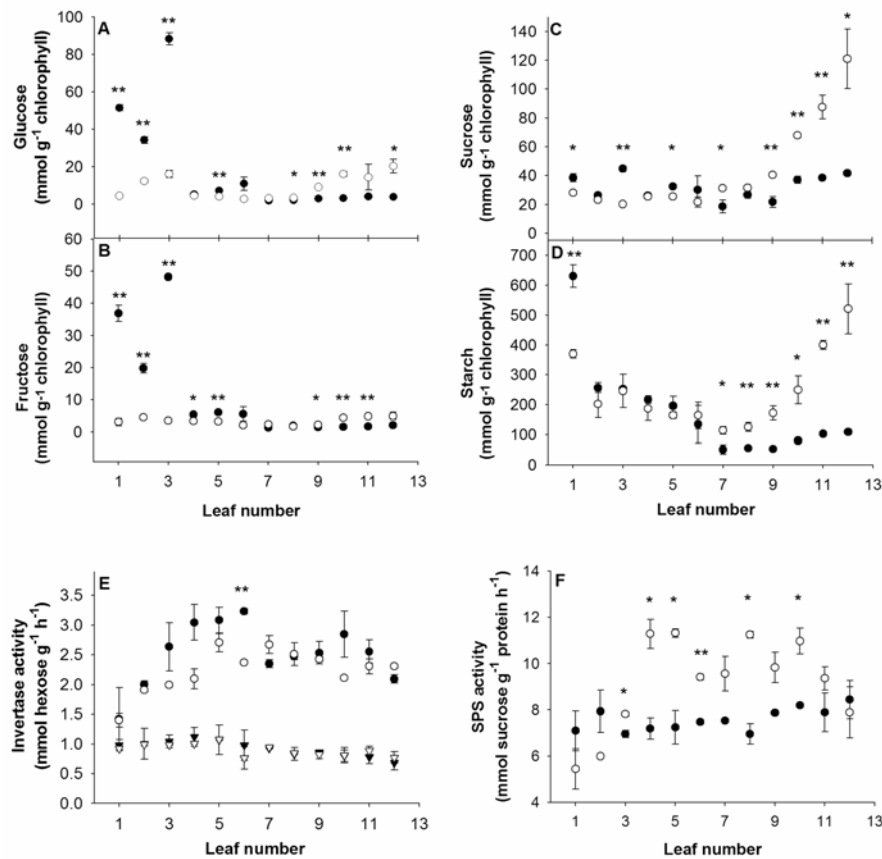
Figure 4.12 Effects of CO_2 enrichment on the abundance of leaf hexoses, sucrose and starch together with the activities of sucrose phosphate synthase and invertase in young and old source leaves. Leaf contents of glucose (A) fructose (B) sucrose (C) and starch (D) and activities of sucrose phosphate synthase (D) and acid invertase (E) were determined in all the leaves of air-grown plants (closed circles) or plants grown with CO_2 enrichment (open circles). Activities of neutral invertase were also determined (E) in all the leaves of air-grown plants (closed triangles) or plants grown with CO_2 enrichment (open triangles). Significant differences at $P < 0.05$ indicated by * and at $P < 0.01$ by **.

Glucose and fructose were greatly increased in the oldest source leaves compared to all other leaves on the stem, which had very low hexose contents when plants were grown in air (Fig. 4.12 A and B). Growth with CO_2 enrichment completely suppressed the age-dependent rise in leaf hexoses such that all the leaves had similar low amounts of glucose and fructose (Fig. 4.12 A). In contrast, while leaf sucrose (Fig. 4.12 C), and starch contents (Fig. 4.12 D) were not greatly affected by leaf rank in plants grown in air, there was a sharp increase in both of these carbohydrates in the youngest source leaves (leaf 7-13) in plants grown with CO_2 enrichment. Soluble acid invertase activities were much higher than those of neutral invertase in all but the oldest leaves on the stem (Fig. 4.12 E). While neutral and acid invertase activities were unaffected by growth CO_2 level (Fig. 4.12

E), SPS activities were markedly increased as a result of growth with CO_2 enrichment, in all but the youngest and oldest leaves (Fig. 4.12 F).

A significant correlation was found between transcript abundance of serpin and hexose content in leaves grown at $350\mu l\ l^{-1}\ CO_2$ (Fig. 4.13), with an r^2 value of 0.77 (p < 0.01) for glucose, and 0.81 (p < 0.01) for fructose. There was a very weak correlation between putative BBI transcript abundance and hexoses, with r^2 values of 0.57 and 0.54 for glucose and fructose respectively. No correlation was found between sucrose content and transcript abundance of either putative serpin or BBI. There was no correlation between transcript abundance of putative serpin or BBI and hexose or sucrose content of leaves grown at $700\mu l\ l^{-1}\ CO_2$ (data not shown).

● Serpin vs glucose; r2=0.77; p=0.0002
○ Serpin vs fructose; r2=0.81; p=0.00006
▼ Serpin vs sucrose; r2=0.08; p=0.3674

● BBI vs glucose; r2=0.57; p=0.0047
○ BBI vs fructose; r2=0.54; p=0.0068
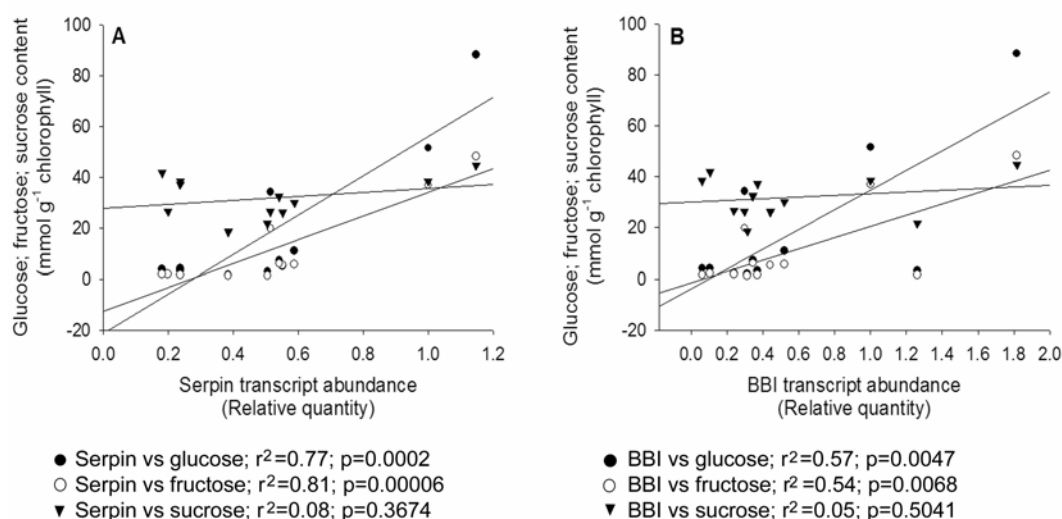▼ BBI vs sucrose; r2=0.05; p=0.5041

Figure 4.13 Correlation between glucose, fructose, and sucrose content and abundance of putative serpin and BBI transcripts. A significant correlation between hexose level and putative serpin transcript abundance was observed (A). A weak correlation between hexose level and putative BBI transcript abundance was observed (B). There was no correlation in either case between sucrose content and transcript abundance.

4.4.7 Modulation of serpin and BBI inhibitor transcripts and transcripts associated with sugar metabolism by sugars and cellular redox modulators

In order to determine the effects of sugars and redox modulators on the expression of the putative serpin and BBI inhibitors, the abundance of putative serpin and BBI transcripts was measured in leaf pieces that had been incubated in solutions containing either sugars (sucrose, glucose or fructose) or pro-oxidants (hydrogen peroxide or methyl viologen; MV; Table 4.8).

Table 4.8 Effects of sugars and pro-oxidants on the abundance of putative serpin and BBI transcripts relative to selected transcripts encoding enzymes of sugar metabolism. Data represent relative minimum-maximum values calculated from at least 3 technical replicates normalised to values obtained from leaves incubated with buffer alone and relative to cyclophilin and ubiquitin as endogenous controls.

		Treatment			
	Sucrose	**Fructose**	**Glucose**	**H_2O_2**	**MV**
Serpin	1.83 (1.64-2.04)	1.59 (1.19-2.12)	1.44 (1.34-1.54)	**2.91** (2.51-3.38)	**7.56** (6.05-9.47)
BBI	**0.54** (0.48-0.61)	**0.52** (0.32-0.85)	**0.44** (0.38-0.51)	**1.97** (1.71-2.27)	1.32 (1.15-1.52)
Incw4	0.96 (0.86-1.07)	0.95 (0.79-1.13)	0.72 (0.67-0.78)	0.78 (0.66-0.92)	0.91 (0.76-1.10)
Inv	0.82 (0.54-1.24)	1.31 (0.96-1.80)	1.04 (0.89-1.21)	**0.32** (0.24-0.42)	0.66 (0.56-0.78)
SuSy3	1.12 (0.94-1.33)	1.29 (1.07-1.55)	1.17 (1.03-1.34)	**0.45** (0.32-0.64)	1.70 (1.52-1.89)
SuSy	1.22 (0.99-1.49)	1.07 (0.72-1.60)	0.72 (0.67-0.77)	1.81 (1.44-2.28)	0.78 (0.62-0.98)
SPS	0.91 (0.74-1.11)	1.18 (1.00-1.40)	0.76 (0.72-0.81)	**0.30** (0.25-0.35)	0.77 (0.67-0.87)

Transcript (row axis label)

Sucrose, fructose, and glucose increased the abundance of serpin transcript and decreased the levels of putative BBI transcripts. Treatment with H_2O_2 and methyl viologen increased the levels of putative serpin transcripts to a similar extent as that observed in the presence of sucrose, fructose or glucose (Table 4.8). However, these pro-oxidants caused a large increase in the abundance of putative BBI transcripts. In contrast, treatment with sugars had very little effect on the abundance of the transcripts associated with sugar metabolism but H_2O_2 and methyl viologen tended to decrease the abundance of these transcripts (Table 4.8).

4.4.8 The effect of leaf position and growth CO_2 level on the abundance of protein carbonyl groups

Using the extent of protein carbonyl group formation as a measure of cellular oxidation, the relationship between leaf rank and cellular redox state was examined (Fig. 4.14).
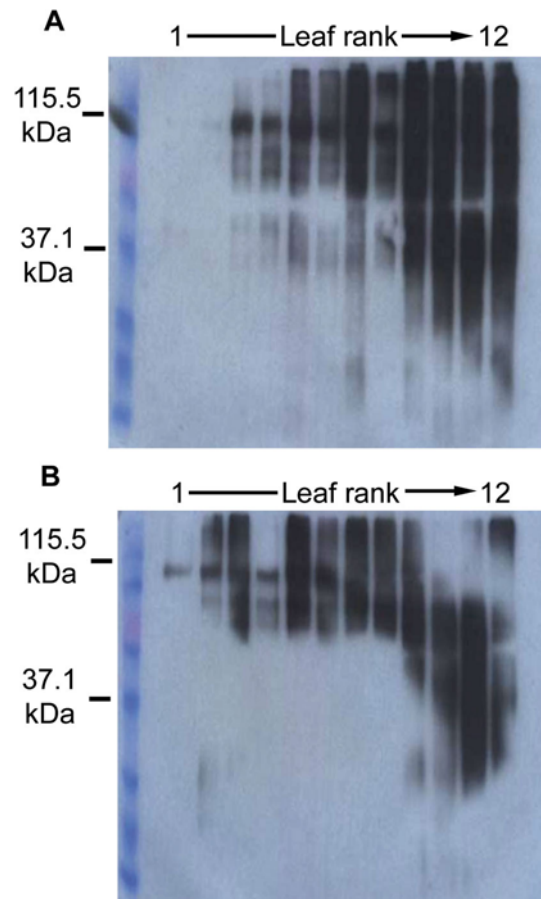
Figure 4.14 Effects of CO_2 enrichment on the abundance of carbonyl groups on the leaf proteins at different positions on the stem of plants grown in air (A) or with CO_2 enrichment (B). The abundance of protein carbonyl groups is compared for all leaves on the stem from the oldest source leaf (leaf rank 1) to the youngest source leaf (leaf rank 12).

Protein carbonyls were most abundant in the youngest source leaves in plants had been grown in air, the number of proteins showing carbonyl group formation and intensity of staining decreasing from the youngest to the oldest source leaves (Fig. 4.14 A). Only one carbonyl-stained protein band was detected in leaf ranks 1 and 2 in air-grown plants (Fig. 4.14 A). Growth with CO_2 enrichment had a dramatic effect on the profile of leaf carbonyl abundance and composition that was particularly marked in the youngest source leaves (Fig. 4.14 B). There was a marked decrease in the number of high molecular weight proteins showing carbonyl group formation in the youngest source leaves at high CO_2 (Fig. 4.14). The level of protein carbonyls was also decreased in other leaf ranks except leaf ranks 1-4 which showed a slight increase compared to the air-grown plants (Fig. 4.14).

4.5 Discussion

The impact of steadily increasing atmospheric CO_2 availability as the major driving force for photosynthesis, carbon gain and whole plant biomass production has become an increasingly important consideration in agriculture for food and bio-fuel production (Long et al., 2004 and 2006). C_4 species are crucial to food security as well as bio-energy applications but their responses to enhanced atmospheric CO_2 availability remains poorly characterized. The data presented here show that growth with CO_2 enrichment did not enhance biomass production or morphology in maize, consistent with other observations (Leakey et al., 2006). These results, however, are in contrast to those observed in Chapter 3, where increased CO_2 availability enhanced plant height. It is likely that the difference in plant height observed in Chapter 3 is due to air-grown maize being grown in cabinets, while high CO_2-grown maize were grown in rooms. This prevented air-grown maize to reach their full height. Growth at the higher CO_2 level furthermore had no significant effects on photosynthesis rates, consistent with previous observations (Leakey et al., 2006). In agreement with these observations, very few transcripts encoding enzymes involved with photosynthesis and primary metabolism were altered by growth at the higher CO_2 level. However, the impact of growth with CO_2 enrichment was dependent on the leaf rank on the stem. Strong development-dependent interactions in the response to CO_2 enrichment involved changes in both leaf carbohydrate status and redox state. We identified two putative serine protease inhibitors that were modulated in response to both of these key regulators of gene expression. We show here that the abundance of transcripts encoding two putative serine protease inhibitors is regulated in response to CO_2 enrichment and that their expression is differentially regulated by sugars, such that putative serpin transcripts were increased in the presence of sucrose, fructose, and glucose while putative BBI transcripts were repressed in the presence of these regulators. The putative serpin (EF406275) that is homologous to an *Arabidopsis* serine-type endopeptidase inhibitor (NP_177351.1) has a theoretical molecular weight of 8.09 kDa and pI of 5.45. The BBI protein has a theoretical molecular weight of 10.4 kDa and pI of 6.01. The putative serpin has a signal peptide and a pin2 domain, while the putative BBI inhibitor has a putative signal peptide and a BB leg domain. The signal peptides suggest that both proteins are targeted to secretary pathways and therefore may be involved in autophagasitic pathways of protein degradation associated with the vesicular transport system.

Entry of proteins into vesicular transport system for degradation from different cellular compartments, such as the chloroplasts and cytosol, was until recently thought only to occur in senescent leaves (Prins et al., submitted for publication to The Plant Cell), is linked to the oxidation of critical amino acids on proteins. The abundance of protein carbonyls on critical amino acids (a measure of cellular oxidation) was highest in the young maize source leaves in air and decreased with leaf position on the stem, such that the oldest source leaves had few detectable carbonyl-containing proteins. This situation appears to be similar to that observed in *Arabidopsis*, where the abundance of protein carbonyl levels progressively increased during vegetative development and then decreased dramatically just prior to bolting and reproductive development (Johansson et al., 2004). While the significance of this development-dependent decrease in protein carbonyl formation remains to be fully elucidated, the data demonstrate that in maize like *Arabidopsis*, protein oxidation is developmentally controlled. Most of the carbonyl groups in young maize leaves were found to be associated with bundle sheath proteins (Kingston-Smith and Foyer, 2000), such as RuBisCO, which is a major target for carbonyl formation upon exposure to oxidative stress (Marin-Navarro and Moreno, 2006). A number of important soluble proteins in leaves, such as RuBisCO and glutamine synthetase, are highly susceptible to oxidation, a process which enhances the cleavage of these proteins (Garcia-Ferris and Moreno, 1994). Within the chloroplast, oxidation of critical cysteine residues enhances the binding of the RuBisCO protein to the chloroplast envelope membranes, marking the protein for degradation (Marín-Navarro and Moreno, 2006). The presence of specific serine protease inhibitors may serve to protect important proteins from turnover in response to appropriate environmental or metabolic cues. A clear correlation between putative serpin transcript abundance and hexose content of leaves grown at 350 µl l^{-1} CO_2 was observed. This supports the role of glucose as signalling molecule, while providing novel evidence for hexoses as possible regulators of serine protease inhibitor expression in maize.

There is no evidence to support the view that oxidative stress was increased in the old source leaves compared to the young source leaves, as the antioxidant transcript profile in the old source leaves reflected adjustments in the defence network rather than a depletion of antioxidant defense. Similarly, the carbonyl groups were lowest in the oldest source leaves and the amounts of leaf anthocyanins were similar in all leaf ranks on the stem and were unaffected by the growth CO_2 environment. However, both the transcriptome profile

and the measured abundance of soluble sugars and starch suggests that there is a massive redeployment of carbohydrate pathways between the young and old source leaves in a manner that was responsive to atmospheric CO_2 availability. Rates of photosynthetic CO_2 assimilation were highest in the young source leaves, where sucrose photosphate synthase transcripts and activity were most abundant. This is consistent with a direct role of the youngest source leaves in carbon gain. Only these leaves accumulated sucrose and starch when plants were grown with CO_2 enrichment. By contrast, the older source leaves, which still maintained high rates of photosynthesis, but showed a high abundance of acid invertase and sugar signaling transcripts, accumulated only hexose when grown with high CO_2. Given the well documented roles of hexoses, hexokinases and the SnRK signaling pathways in controlling gene expression in response to both external environmental and metabolic cues (Baena-González et al., 2007), it can be concluded that the transcriptome signature of the older leaves is consistent with the operation of the sugar-mediated hexokinase signally pathway in the control of the two high CO_2-modulated putative serine protease inhibitors identified in this study.

In this part of the study it was demonstrated that high CO_2–dependent and hexose-dependent control of two putative serine protease inhibitors that participate in the network controlling protein stability and turnover underpins the acclimatory responses to growth CO_2 availability. Similarly, the enhanced operation of sugar signaling pathways in the older source leaves observed in this study is entirely consistent with observations of long distance signaling of information regarding CO_2 availability from mature to developing leaves (Lake et al., 2001). While long-distance CO_2 signaling systems involve sugars and similar molecules (Coupe et al., 2006; Miyazawa et al., 2006), the CO_2 signaling pathways that influence key parameters, such as absolute stomatal numbers and stomatal function (Lake et al., 2002; Woodward, 2002), remain poorly characterized with few identified regulators (Gray et al., 2000).